Atmospheric Environment 246 (2021) 118113

Contents lists available at ScienceDirect

Atmospheric Environment

journal homepage: http://www.elsevier.com/locate/atmosenv

Evaluating oil and gas contributions to ambient nonmethane hydrocarbon mixing ratios and ozone-related metrics in the Colorado Front Range

Congmeng Lyu [a], Shannon L. Capps [a,*], Kent Kurashima [b], Daven K. Henze [b], Gordon Pierce [c], Amir Hakami [d], Shunliu Zhao [d], Jaroslav Resler [e], Gregory R. Carmichael [f], Adrian Sandu [g], Armistead G. Russell [h], Tianfeng Chai [i], Jana Milford [b]

[a] Department of Civil, Architectural, and Environmental Engineering, Drexel University, Philadelphia, PA, 19101, USA
[b] Department of Mechanical Engineering, University of Colorado, Boulder, CO, 80310, USA
[c] Colorado Department of Public Health and Environment, Denver, CO, 80246, USA
[d] Department of Civil and Environmental Engineering, Carleton University, Ottawa, ON, K1S 5B6, Canada
[e] The Czech Academy of Sciences, Institute of Computer Science, Prague, Czech Republic
[f] Department of Chemical and Biochemical Engineering, University of Iowa, Iowa City, IA, 52242, USA
[g] Computer Science, Virginia Polytechnic Institute and State University, Blacksburg, VA, 24060, USA
[h] School of Civil and Environmental Engineering, Georgia Institute of Technology, Atlanta, GA, 30332, USA
[i] NOAA Air Resources Laboratory; Cooperative Institute for Satellite Earth System Studies (CISESS), University of Maryland, College Park, MD, 20742, USA

HIGHLIGHTS

- Oil & natural gas (O&NG) contributions to air pollution were less in 2015 than 2013.
- Vehicular contributions were most substantial in Denver and changed less over time.
- Estimated ozone-related mortality was greatest from O&NG and vehicular emissions.

ARTICLE INFO

Keywords:
Oil and natural gas
Nonmethane hydrocarbon
Ground-level ozone
Premature mortality
Source apportionment
Adjoint sensitivity analysis

ABSTRACT

Recently, oil and natural gas (O&NG) production activities in the Denver-Julesburg Basin have expanded rapidly. Associated nonmethane hydrocarbon (NMHC) emissions contribute to photochemical formation of ground-level ozone and include benzene as well as other hazardous air pollutants. Using positive matrix factorization (PMF) and chemical mass balance (CMB) methods, we estimate how much O&NG activities and other sources contribute to morning NMHC mixing ratios measured from 2013 to mid-2016 at a site in Platteville, CO, in the Denver-Julesburg Basin, and at a contrasting site in downtown Denver. A novel adjoint sensitivity analysis method is then used to estimate corresponding contributions to ozone and ozone-linked mortality in the Denver region. Average 6–9 am NMHC mixing ratios in Platteville were seven times higher than those in Denver in 2013 but four times higher in 2016. CMB estimates that O&NG activities contributed to the Platteville (Denver) site an average of 96% (56%) of NMHC on a carbon basis while PMF indicated 92% (33%). Average vehicle-related contributions of NMHC are estimated as 41% by CMB and 53% by PMF in Denver. Estimates of the fractional contribution to potential ozone and ozone-linked mortality from O&NG activities are smaller while those from vehicles are larger than the NMHC contributions. CMB (PMF) indicate that greater than 78% (40%) of annual average benzene in Denver is attributable to vehicle emissions while greater than 75% (67%) of benzene in Platteville is attributable to O&NG activities.

1. Introduction

Over the past decade, oil and natural gas (O&NG) production activities in the Denver-Julesburg (DJ) Basin have emerged as a significant air pollution source in northeastern Colorado, where summertime levels of ground-level ozone exceed federal air quality standards (Air

* Corresponding author.
E-mail address: shannon.capps@drexel.edu (S.L. Capps).

https://doi.org/10.1016/j.atmosenv.2020.118113
Received 14 May 2020; Received in revised form 11 November 2020; Accepted 27 November 2020
Available online 15 December 2020

Pollution Control Division, 2017). O&NG production activities contribute emissions of nonmethane hydrocarbons (NMHC) and nitrogen oxides (NOx), which are both ozone precursors (Schnell et al., 2009). Exposure to ambient ozone is associated with human mortality (Turner et al., 2016) with Vos et al. (2020) estimating that 0.43% of deaths by all causes in the United States were attributable to this risk factor in 2019. Rapid growth in oil and gas production in close proximity to residential areas has also prompted increased research into hazardous air pollutant emissions, including benzene, toluene, ethylbenzene, and xylenes (BTEX) (McKenzie et al., 2018).

The Denver Metro/North Front Range ozone nonattainment area (NAA) is comprised of Adams, Arapahoe, Boulder, Broomfield, Denver, Douglas, and Jefferson counties along with parts of Larimer and Weld counties (Regional Air Quality Council, 2016). The total population in the area from the 2010 census was 3.35 million, with additional growth since then (U. S. EPA, 2018). Oil production in the nine NAA counties increased by a factor of eight from 2006 to 2016, with 106 million barrels produced in 2016 (COGCC, 2017). Natural gas production increased by a factor of three over the same period, with 641 billion cubic feet produced in 2016 (COGCC, 2017). For both commodities, about 98% of this production was in Weld County, to the northeast of the Denver Metro area. The emissions inventory developed by the state of Colorado for the year 2017 estimates that O&NG sources emitted 154 tons per day (TPD) of volatile organic compounds (VOC) in the NAA, representing 44% of the area's anthropogenic VOC emissions (Wells, 2017).

In response to increasing O&NG activity and concerns about ozone nonattainment, in 2004, 2008, 2014, and 2017 Colorado adopted a sequence of increasingly stringent control requirements for sources in the O&NG sector (CDPHE, 2017; Milford, 2014; Wells, 2017). The U.S. Environmental Protection Agency (EPA) adopted nationally applicable new source performance standards for O&NG sources in 2012 (U. S. EPA, 2012) with additional regulations adopted in 2016 (U. S. EPA, 2016a). At the same time, operators in northeastern Colorado have updated their equipment and practices. As a result, while production has continued to increase, the state of Colorado estimates of VOC emissions per unit of oil or gas produced have declined (Wells, 2017).

Emissions inventory estimates, such as those of Wells (2017), are developed using engineering estimation techniques, involving sampling or modeling a subset of sources to develop emissions factors; operator surveys to estimate equipment counts and other activity factors; and use of engineering judgment to estimate the effectiveness of emissions control requirements. Accordingly, these estimates are subject to a number of uncertainties, including the representativeness of sampling and survey results, unanticipated gaps in implementation of control requirements, and changing practices that are not reflected in the original estimates. These uncertainties have motivated a number of past efforts to evaluate or constrain NMHC emissions or source contribution estimates using observations and statistical analysis or modeling.

As one of the earlier investigations of O&NG contributions in the region, Pétron et al. (2012) analyzed hydrocarbon mixing ratio data measured from 2007 to 2010 at the Boulder Atmospheric Observatory (BAO) tower near Erie, CO (40.05°N, 105.00°W) together with flask samples obtained around northeastern Colorado in June–July 2008. They concluded that available inventories underestimated emissions of methane, n-butane, isomers of pentane, and benzene, all of which are likely associated with O&NG activities (Shah et al., 2015; U. S. EPA, 1998). Subsequently, Gilman et al. (2013) performed source apportionment by applying multivariate regression to in-situ hydrocarbon measurements made at the BAO tower from February 18 – March 7, 2011. They estimated that O&NG emissions contribute 70% or more of measured C_2 – C_7 alkanes and about 20–30% of benzene, toluene, and xylene. By weighting with hydroxyl radical reaction rate constants (k_{OH}), they estimated O&NG sources contributed an average of 55% to the reactivity of the NMHC mixture. For the same time period in 2011, Swarthout et al. (2013) determined through wind profile analysis that natural gas production was the main source of elevated alkane mixing ratios measured in canister samples at the BAO tower, and that urban combustion emissions were more likely to have contributed to elevated alkene mixing ratios.

Measurements conducted in 2012 and 2013 were the basis for additional studies. Pétron et al. (2014) applied mass balance methods and multivariate regression to methane and NMHC measurements from aircraft flights on May 29 and 31, 2012, to make "top down" estimates of O&NG emissions in a 70 km by 85 km region roughly centered on Platteville, CO. Their analysis suggested that the state's inventory underestimates C_3 – C_5 alkane emissions from O&NG sources by a factor of two and that O&NG emissions of benzene equal or exceed the contribution from mobile sources. McDuffie et al. (2016) estimated the contribution of O&NG to ozone formation using a photochemical box model, with mixing ratios of C_2 – C_{10} hydrocarbons, C_2 – C_4 oxygenated VOC, and NOx measured at the BAO tower in July and August 2012 as model inputs. They estimated that O&NG VOC emissions contributed just under 20% of locally produced ozone, even though they contributed over 70% of the total nonmethane organic compounds on a carbon mixing ratio basis. Thompson et al. (2014) measured NMHC mixing ratios between March and June 2013 at seven locations near residences or farms in Erie and Longmont, CO. They attributed the elevated levels of ethane, benzene, and other light alkanes they observed to O&NG activities, in part because the ratio of i-pentane to n-pentane closely matched the ratio from raw natural gas.

Multiple studies conducted as part of the FRAPPE and DISCOVER-AQ field campaign conducted in summer 2014 addressed O&NG contributions to NMHC and ozone (Flocke et al., 2020). Of particular relevance here, at a site 9 km southeast of Platteville, Halliday et al. (2016) observed elevated benzene mixing ratios during the field campaign, and found that benzene was highly correlated with the O&NG tracers propane, pentanes, and n-butane, and weakly correlated with the combustion tracers carbon monoxide and acetylene. Pfister et al. (2017) applied the WRF-CMAQ atmospheric chemistry and transport model to evaluate the CO, NOx and VOC inventories for the North Front Range metropolitan area (NFRMA) by comparing model results to aircraft and surface observations made in July and August 2014. They found that the prior estimates of VOC emissions from O&NG sources were too low to account for observed levels of compounds other than ethane and recommended a factor of two (or greater) adjustment. They also concluded that mobile sources and oil and gas emissions were the largest contributors to local ozone production in the region.

Using VOC mixing ratios measured at the BAO tower during spring and summer 2015, Abeleira et al. (2017) identified source contributions with Positive Matrix Factorization (PMF). They identified the main PMF factors as long-lived O&NG emissions, short-lived O&NG, traffic, background, secondary, and biogenics (summer only). The long-lived O&NG factor accounted for 36%–100% of the observed C_2–C_6 alkanes. The short-lived O&NG factor was comprised largely of C_7 and C_8 alkanes, while the traffic factor accounted for most of the ethyne (acetylene), aromatics, and larger alkanes. The O&NG factors accounted for more than 70% of the observed benzene, 30–40% of the toluene, and about 40–70% of the k_{OH}-weighted VOC reactivity (including both NMHC and oxygenated VOCs).

In this study, we use PMF and chemical mass balance (CMB) methods to estimate how much O&NG sources contribute to 6–9 am measurements from January 2013 to June 2016 of total NMHC, benzene, and toluene at two contrasting locations in northeastern Colorado. The first site is in Platteville, a small town in southwestern Weld County that is located in the heart of O&NG activity in the DJ Basin. The second monitoring location is in the urban core of Denver. Use of both PMF and CMB allows us to assess the robustness of the results to the distinct assumptions made with each source apportionment technique. Conducting source apportionment with these more recent measurements over a period of years is designed to augment investigations made with measurements from earlier time periods and to provide insight into how

the changes of practices by Colorado O&NG producers may have influenced emissions. We then use sensitivity analysis conducted with the CMAQ adjoint to study the relative contributions each of the PMF factors or CMB sources makes to daily maximum 8-h average (MDA8) ozone and ozone-related premature mortality in the 12-county Denver Combined Statistical Area (CSA) (Table S.1). CMB and sensitivity analysis with the CMAQ adjoint have not previously been applied to inform the influence of O&NG emissions on NMHC mixing ratios nor ozone and its health impacts in the Colorado Front Range. Furthermore, to the knowledge of the authors, this is the first time PMF and CMB source apportionment results have been combined with high resolution CMAQ adjoint sensitivities to extend the source apportionment results from direct contributions to primary NMHC to estimate contributions to a secondary pollutant, ozone, and its associated health risks.

2. Methods

2.1. Measurements and data preparation

The Colorado Department of Public Health and the Environment (CDPHE) began the Ozone Precursor Study (OPS) in December 2011 to observe morning (6:00 to 9:00 am Mountain standard) mixing ratios of organic gases at two distinct sites to help understand what sources might be contributing to ozone formation along the Front Range. This ongoing study collects data once every six days, year-round. The 6–9 am sampling time period was selected to focus on emissions from anthropogenic compounds during typically low mixing height conditions and prior to significant photochemical activity. Consequently, the sampling period is biased with respect to biogenic compounds with light and temperature dependent emissions that typically increase later in the day. The 6–9 am sampling period also represents relatively local influences, due to typically light winds and limited atmospheric mixing. The Denver measurement site is located at the CAMP air monitoring station (Air Quality System [AQS] #08-031-0002) at 2105 Broadway St, Denver, CO, (39.75°N, −104.99°W) at an elevation of 1593 m. The Platteville measurement site is located at Platteville Middle School at 1004 Main Street, Platteville, CO, (40.21°N, −104.82°W) at an elevation of 1469 m. More information about the sampling sites is provided in the Supplemental Material, Section S.2. Hereinafter, for ease of reference these specific locations are identified simply as “Denver” and “Platteville”. Figure S.1 provides a map showing the monitoring locations and their proximity to O&NG well sites in the DJ Basin. From December 2011 to June 2016, Eastern Research Group (ERG) in Morrisville, NC, was contracted to provide the sampling supplies and conduct analyses. The study is ongoing but has used a new analytical laboratory, Atmospheric Analysis & Consulting (AAC), since July 2016. This study focuses on data collected from 2013 through June 2016, to ensure consistency in sampling and analysis procedures. The complete OPS data are available at https://www.colorado.gov/airquality/tech_doc_repository.aspx#special_studies.

In the OPS, time-integrated samples are collected in Summa canisters. Duplicate samples are obtained with at least one-in-ten frequency to assess method precision (CDPHE, 2018). Canisters are cleaned prior to deployment at monitoring sites using pressure-vacuum cycling with a humidified nitrogen purge and heat treatment, with batch blank analysis conducted to ensure adequate cleaning (ERG, 2016). Air from the Summa canisters was analyzed for NMHCs with EPA Compendium Method TO-15 (U. S. EPA, 1999) following ERG’s documented quality assurance project plan (ERG, 2015). The TO-15 method provides for the concurrent analysis of samples by gas chromatography with mass spectrometry as well as optional flame ionization detection and selected ion monitoring (SIM) (GC/MS with optional FID). Samples were analyzed within 30 days of collection, ensuring stability for most target NMHC (Kelly and Holdren, 1995 and references therein). However, canister losses cannot be ruled out for unsaturated NMHC such as isoprene that can react with ozone in the air being sampled. Additional information on sampling and analysis methods and quality assurance is provided in the Supplemental Material, Section S.2. Accordingly, measurements of 79 NMHC and their detection limits according to the appropriate method from January 2013 through June 2016 were considered for inclusion in this work.

The OPS data were preprocessed before being utilized in CMB or PMF. Time series and pairwise correlations were examined to screen for potential outliers and artifacts (Fig. S.2-5). Data for April 10, 2013, and February 16, 2014, in Platteville were removed from the data set due to extremely high measurements of isobutane. No other full days were removed, but if a species fell below the minimum detection limit (MDL) for greater than 60% of observations at a specific site throughout the January 2013 to June 2016 period, then the species was removed from the data set. After preprocessing, 370 observations of 49 compounds were ultimately included in the source apportionment analysis. Estimated detection limits are provided in Table S.2 for the full set of 79 NMHC measured in the OPS, and the number of occurrences of observations below these limits are provided for compounds included in CMB and PMF. Table S.3 shows the agreement between collocated samples for the 49 compounds included in the source apportionment analysis. For measurements above the MDL, the mixing ratios used in source apportionment were directly from the measurements taken in the OPS. If the reported mixing ratio was below the MDL, then the mixing ratio provided to the source apportionment models was half the value of the MDL, which Polissar et al. (1998) recommended and Brown et al. (2007) applied to apportionment of ozone precursors. The uncertainty was calculated based on the MDL determined by EPA Compendium Method TO-12 and an additional ten percent error fraction (EF) (Eq. (1)) (Norris et al., 2014).

$$unc = \left\{ \frac{5}{6} MDL \ if \ conc \le MDL, \sqrt{(EF{*}conc)^2 + (0.5MDL)^2} \ if \ conc > MDL \right\} \quad (1)$$

2.2. Chemical mass balance model

The CMB model has long been used to apportion particulate matter (Watson et al., 1984) and VOCs (e.g., Fujita et al., 1995; Harley et al., 1992; Scheff and Wadden, 1993). CMB uses a weighted least squares solution to quantify the contribution of pre-specified sources to receptor measurements. The CMB model solves the equation:

$$C_{q,l,t} = \sum_{u=1}^{U} F_{q,u} \cdot S_{u,l,t} + \varepsilon_{q,l,t} \quad q = 1, 2, 3 \ldots n \quad (2)$$

In Eq. (2), $C_{q,l,t}$ represents the mixing ratio of species q of the n NMHCs measured at location l at time t; F_{qu} represents the fraction of species q in emissions from source u; $S_{u,l,t}$ represents the estimate of the contribution from source u at location l at time t; and $\varepsilon_{q,l,t}$ denotes the residual error for species q at location l at time t. A unique solution can be obtained for Eq. (2) when the number of species measured, n, is equal to or greater than the number of sources, U. In this study, seven or eight sources (architectural coatings, vehicle exhaust, diurnal evaporative emissions, produced gas, condensate tanks, isoprene, alpha-pinene, and propane) were used to explain the measured pollutant mixing ratios, while 49 NMHC species were studied, which are listed in Table S2. Eq. (2) is solved simultaneously by an effective variance weighted solution. The weights reflect the uncertainty in both the ambient mixing ratios and the source profiles. The EPA-CMB8.2 model was used for this study (Coulter, 2004).

CMB requires advanced specification of sources and associated chemical speciation profiles. To identify sources that should be included in the CMB analysis, we used the 2011 VOC emissions inventory developed by CDPHE for the Denver Metro/North Front Range (Wells, 2017). Candidate chemical speciation profiles for the identified sources were obtained from EPA’s SPECIATE v4.5 repository (U. S. EPA, 2016b),

from local studies of oil and gas emissions, and from the literature. Selection of profiles took into account their completeness and relevance to the Colorado location and the 2013–2016 timeframe. The final profiles, which are briefly described in Table 1, were selected after extensive testing of alternative combinations to avoid problems with collinearity and non-convergence of CMB solutions and to maximize model performance based on percent mass accounted for, R^2, and χ^2 metrics. Note that seasonal variation in profiles is likely due to temperature changes inducing different rates of evaporation for chemicals with distinct vapor pressures. However, the vehicular source profiles are the only ones available that include a range of temperatures whereas such sophisticated profiles are not available for the O&NG activity profiles. Profiles for isoprene, α-pinene, and propane were comprised exclusively of the compound by which they are named. Alternative profiles considered for oil and gas sources are compared in the Supplemental Material, Section 6. Compared to the alternatives, the chosen profiles for condensate tank emissions and produced gas were relatively complete in speciation and provided distinct source apportionment without excessive collinearity. The vehicle exhaust and evaporative emission profiles used were the most recent available for gasoline with RVP and ethanol content comparable to fuels used in the Colorado Front Range. Where multiple profiles were reported in a given study, uncertainties in species carbon fractions were estimated as the standard error of the mean. When only aggregate profiles were reported, a relative uncertainty of 35% was assumed for the carbon fractions as a default. Additional details about these profiles and the basis for their selection are provided in Kurashima (2018).

2.3. Positive matrix factorization

PMF is a multivariate factor analysis tool, initially developed by Paatero and Tapper (1994) with further development by EPA, which factors a speciated sample data matrix into a factor contributions matrix and a factor profiles matrix (Norris et al., 2014). PMF has been widely used for the source apportionment of VOCs (e.g., Brown et al., 2007; Jorquera and Rappenglück, 2004; Leuchner and Rappenglück, 2010) as well as particulate matter (e.g., Hasheminassab et al., 2014; Kim and Hopke, 2004; 2008; Zhang et al., 2009). PMF finds a constrained, weighted least squares solution to

$$E_{q,l,t} = \sum_{r=1}^{p} A_{q,r} B_{r,l,t} + \varepsilon_{q,l,t} \quad q = 1,\ 2,\ \ldots, n \tag{3}$$

where $E_{q,l,t}$ represents the predicted concentration of compound q of the n NMHCs measured at location l at time t; $A_{q,r}$ represents the loading of compound q on factor r (factor profile); $B_{r,l,t}$ is the r^{th} factor score (normalized factor contribution) for the total mixing ratio at location l at time t; and $\varepsilon_{q,l,t}$ denotes the residual error for compound q at location l at time t. The number of factors, p, is chosen by the user. PMF minimizes a weighted sum of squares incorporating error estimates for the data with factors constrained to be nonnegative. Since a large number of solutions may satisfy the nonnegative constraint, the stability of the resulting factors was further evaluated through rotational perturbation.

Measurements from both locations were treated as a single, unified set of inputs to PMF. This joint analysis caused the factors identified by PMF to be identical for Denver and Platteville. The preprocessed data were analyzed in two stages with the U.S. EPA's Positive Matrix Factorization v.5 software (Norris et al., 2014). Any observations that were missing due to the measurement techniques or preprocessing were indicated to PMF as such in place of an observation. The sum of the identified NMHCs was indicated to PMF as the total, so the sum is a weak constraint.

Table 1
Source profiles used in CMB modeling.

Source	Origin	Note
Condensate Tanks	Brantley et al. (2015)	27 canister samples representing condensate tanks from the DJ Basin
Produced Gas	Shah et al. (2015)	Western Regional Air Partnership survey of O&NG companies in the DJ Basin (data from 2006)
Vehicle Exhaust	U. S. EPA (2009)	San Antonio, TX; three 2008 vehicles; 10% ethanol gasoline; Reid Vapor Pressure (RVP) 9.0 psi
Diurnal Evaporative Emissions	Haskew (2010)	San Antonio, TX. Eight vehicles, model years 2000–2004. RVPs 7.0 psi and 10.0 psi, Temperature modulated from 65 °F to 105 °F
Architectural Solvents	State of California Air Resources Board (1997)	Survey of aerosol coating manufacturers and marketers selling products in California

2.4. CMAQ adjoint modeling

The Community Multiscale Air Quality (CMAQ) model is widely used to study the relationship of secondary air pollutants such as ozone to emissions of precursor pollutants such as NMHCs and NOx. With a linearized approximation, the adjoint of CMAQ (Hakami et al., 2007; Sandu and Sander, 2005; Zhao et al., 2020) provides the influence of each input parameter on a concentration-based metric. In this version of the CMAQ adjoint, the gas phase chemical mechanism is CB-05 (Yarwood et al., 2005). Emissions are based on the 2008 National Emissions Inventory v2 projected back to 2007 (Rao et al., 2013) and the Motor Vehicle Emission Simulator (MOVES) v2010b projected back to 2007 (U. S. EPA, 2014). Meteorology for the year 2007 is modeled with the Weather Research and Forecasting (WRF) model v3.1 (U. S. EPA, 2011; Skamarock et al., 2005). The model is applied to 82 rows and 132 columns of 36-km by 36-km horizontal resolution grid cells over the continental U.S. with pressure-following vertical layers. Other details of the CMAQ adjoint model configuration and evaluation of ozone performance, which was reasonable, can be found in Lyu et al. (2019).

One way to estimate the potential contribution of ozone precursors to ozone formation and associated health risks is to employ adjoint-based mixing ratio gradients, $\frac{\partial J}{\partial MR_{i,l,t}}$, which are the species-, location-, and time-specific sensitivities quantified by the adjoint model, where i is the species index, l is the grid cell index, and t is the time index. The numerator, J, is a cost function that may be composed of any concentration-based metric. The denominator, $MR_{i,l,t}$, is the mixing ratio of an ozone precursor at a certain location l and time t. The calculations of adjoint-based mixing ratio gradients are explained in Section S.3.1.

Relative influences of NMHCs on the cost function, J, for the r^{th} factor from PMF, $\mathbb{C}_{r,l,t}$, or for the u^{th} source from CMB, $\mathbb{C}_{u,l,t}$, are estimated (Eq. (4) and (5)).

$$\mathbb{C}_{r,l,t} = \sum_{i} \frac{\partial J}{\partial MR_{i,l,m}} \boldsymbol{X}_{q,i} \frac{A_{q,r} B_{r,l,t}}{J} \tag{4}$$

$$\mathbb{C}_{u,l,t} = \sum_{i} \frac{\partial J}{\partial MR_{i,l,m}} \boldsymbol{X}_{q,i} \frac{F_{q,u} \cdot S_{u,l,t}}{J} \tag{5}$$

where $\frac{\partial J}{\partial MR_{i,l,m}}$ represents the average adjoint-based mixing ratio gradients for the m^{th} month for the CB05 species i at location l (Section S.3.2); $\boldsymbol{X}_{q,i}$ represents the matrix that relates each observed NMHC q to the corresponding CB05 species i (Section S.3.3); $A_{q,r}B_{r,l,t}$ represents the PMF-based contribution of factor r at location l at time t for the observed NMHC q; and $F_{q,u} \cdot S_{u,l,t}$ represents the CMB-based contribution of source u at location l at time t for the observed NMHC q.

To estimate the relative contribution of ozone precursors to ozone formation and associated health risks, we selected the absolute maximum daily 8-h average (MDA8) ozone and ozone-related premature mortality in the Denver CSA as cost functions. The Denver CSA includes Denver, Boulder, and Weld counties, along with nine other

counties included in the Denver-Aurora-Lakewood Metropolitan Statistical Area (Table S1). The MDA8 ozone cost function is the temporal and spatial average of MDA8 ozone in the Denver CSA grid cells from March through August, the period when monthly average MDA8 are highest in the Denver CSA for the modeled year. Average MDA8 cost function gradients are calculated for each month in each grid cell from March through August (Section S.3.2). These monthly average sensitivities are used to calculate relative influences of PMF factors $\mathbb{C}_{r,l,t}$ and CMB sources $\mathbb{C}_{u,l,t}$ on each cost function (Eq. (4) and (5); Section S.3). The ozone-related premature mortality is represented with the exposure-response model developed by Turner et al. (2016) that has a concentration response factor, β, as 0.0198 per 10 ppb. This cost function accounts for the annual all-cause premature mortality in the Denver CSA attributable to long-term ozone exposure above a theoretical minimum risk exposure level (TMREL) (Cohen et al., 2017; Liang et al., 2018; Lim et al., 2014), which is set at 28.9 ppb by taking the average of the two low concentration cutoff values for North America in Malley et al. (2017). This premature mortality cost function is the same as that used by Lyu et al. (2019), except for its application to the smaller geographic region of the Denver CSA rather than the continental US.

$$M = \sum_{l=1}^{N} M_{0(l)}(1 - e^{-\beta \Delta c_{(l)}}), \tag{6}$$

where N is the number of grid cells in the Denver CSA, $M_{0(l)}$ (deaths/year) represents the gridded annual non-accidental baseline mortality in the Denver CSA for people age 30 or older in 2010 (U. S. EPA, 2013) and for each grid cell, $\Delta c_{(l)}$ is calculated as:

$$\Delta c_{(l)} = \begin{cases} c_{(l)} - TMREL, & if\ c_{(l)} > TMREL \\ 0, & if\ c_{(l)} \leq TMREL \end{cases} \tag{7}$$

where $c_{(l)}$ is the annual mean of the MDA8 ozone in each grid cell. The impacts of the mismatch in time between the CMAQ model scenario in 2007, the population data from 2010, and the observations from 2013 to 2016 are somewhat limited by assessing only the relative influences. Additionally, the emissions of NOx and NMHC in the 2014 NEI are within 10% of those from the 2008 NEI (Table S.4), which is smaller than the 30% range within which these sensitivities are considered useful. Furthermore, the meteorological conditions reflected in temperature and precipitation reflect reasonably small differences between 2013 to 2015 and 2007 (Fig. S.6,7). These assessments suggested that combining adjoint-based sensitivities with apportioned observations from the OPS study was reasonable.

3. Data

The average and standard deviations of the ambient mixing ratios of selected NMHCs for each year depict the differences between Denver and Platteville (Table 2). On average, the ambient NMHC mixing ratios (*ppb C)* at Platteville are 5.5 times greater than those in Denver. A few species such as benzene, toluene, acetylene, ethylene, cis-2-butene, and trans-2-butene are relatively similar in both Denver and Platteville, and the mixing ratios for each of the aforementioned species constitutes less than 10% of the total NMHC mixing ratio on average. Mixing ratios of ethane, propane, and n-butane in Platteville are much larger than the mixing ratios measured in Denver. As expected, these differences between locations are consistent with the analysis of Thompson et al. (2014) of the 2013 CDPHE NMHC observations. The means of the total mixing ratio are lower in both locations in January through June of 2016 compared to the same six-month period in 2013 though the 95% confidence intervals overlap for the Denver site (Fig. 1). The mean NMHC mixing ratios in Denver decreased to a minimum for January through June of 2014; subsequently the six-month mean of the total NMHC mixing ratio increased but remained below the 2013 six-month means (Fig. 1). Platteville saw significantly lower ($p < 0.05$ for one-sided student's t-test) annual mean NMHC mixing ratios in 2014 and 2015 compared to 2013. Additionally, the six-month mean of the total NMHC mixing ratio for January through June of 2016 was lower than any other six-month period with a 95% confidence interval that does not cross the 2013a or 2013b confidence intervals (Fig. 1). Not all individual species have lower mixing ratios in the final six-month period of observations.

Table 2
Statistical description of the CDPHE data used in this study. The number of samples, *N*, as well as the average and standard deviation of NMHC mixing ratios (ppb C(v)) at the Denver site and the Platteville site, by year or six-month period.

Site	Denver				Platteville			
Year	2013	2014	2015	2016a*	2013	2014	2015	2016a*
N	56	58	48	31	45	56	48	28
Total	164.4 ±97.3	128.5 ±72.7	143.9 ±67.5	137.5 ±98.9	1129.6 ± 813.4	751.9 ±563.2	688.8 ±457.1	572.6 ±392.6
benzene	2.9 ±1.7	2.2 ±1.6	2.2 ±1.0	2.4 ±1.9	5.1 ±3.4	3.7 ±2.4	3.7 ±2.1	3.8 ±3.2
toluene	9.0 ±4.8	8.7 ±6.5	8.2 ±4.8	7.3 ±5.4	8.5 ±4.8	7.1 ±4.7	7.1 ±4.2	6.3 ±3.9
ethane	29.6 ±23.5	22.8 ±16.5	28.2 ±18.5	32.9 ±25.4	250.5 ±204.1	160 ±121.6	155 ±108.9	137 ±93.4
propane	21.5 ±17	16.5 ±12.2	16.6 ±11.9	14.6 ±9.6	284.5 ±210.7	190.5 ±144.7	173.2 ±117.1	145.2 ±105.8
n-butane	14 ±11.3	10.9 ±8.5	11.8 ±8.9	12.1 ±11.8	186.2 ±140.2	122.2 ±94.4	107.4 ±71.8	87.3 ±61.4
isobutane	5.8 ±4.5	4.6 ±3.3	5.5 ±4.6	4.8 ±4.3	78.9 ±60.6	49.7 ±38.9	43.7 ±30.1	37.1 ±26.9
n-hexane	3.6 ±2.0	3.3 ±1.7	3.8 ±1.7	3.3 ±1.9	23 ±16.3	20 ±14.3	18.2 ±11.3	14.2 ±9.2
acetylene	4.8 ±4.2	3.8 ±3.6	3.7 ±2.5	3.8 ±3.7	2.9 ±2.7	2.1 ±1.8	2.8 ±2.5	3.3 ±2.9
ethylene	7.4 ±5.3	6.2 ±4.2	6.2 ±3.6	5.9 ±4.9	6.0 ±3.9	4.4 ±2.4	4.7 ±3.7	4.5 ±3.3
cis-2-butene	0.3 ±0.2	0.2 ±0.2	0.2 ±0.1	0.2 ±0.2	0.3 ±0.3	0.1 ±0.2	0.2 ±0.2	0.2 ±0.2
trans-2-butene	0.4 ±0.3	0.3 ±0.3	0.4 ±0.7	0.3 ±0.3	0.4 ±0.3	0.2 ±0.2	0.2 ±0.2	0.3 ±0.2

Note: "Total" represents the sum of the 49 compounds included in the study. *2016a indicates that the measurements in 2016 concluded at the end of June.

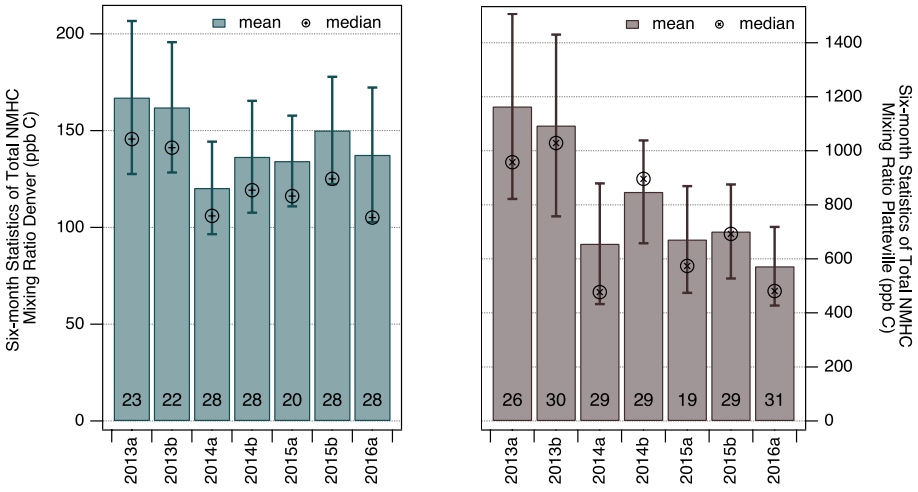

Fig. 1. Summary statistics for six-month periods of 6–9 am total NMHC observed. The left panel represents the observations at Denver with the right panel reflecting Platteville observations. The "a" period of a year includes January through June observations while the "b" indicates July through December observations. The number of observations in each six-month period are indicated as a black number at the base of each bar. The mean is indicated by the height of the bar, corresponding to the respective y-axis. The median is indicated by the black circle with a centered "x". The 95% confidence interval is indicated by the bars about each mean.

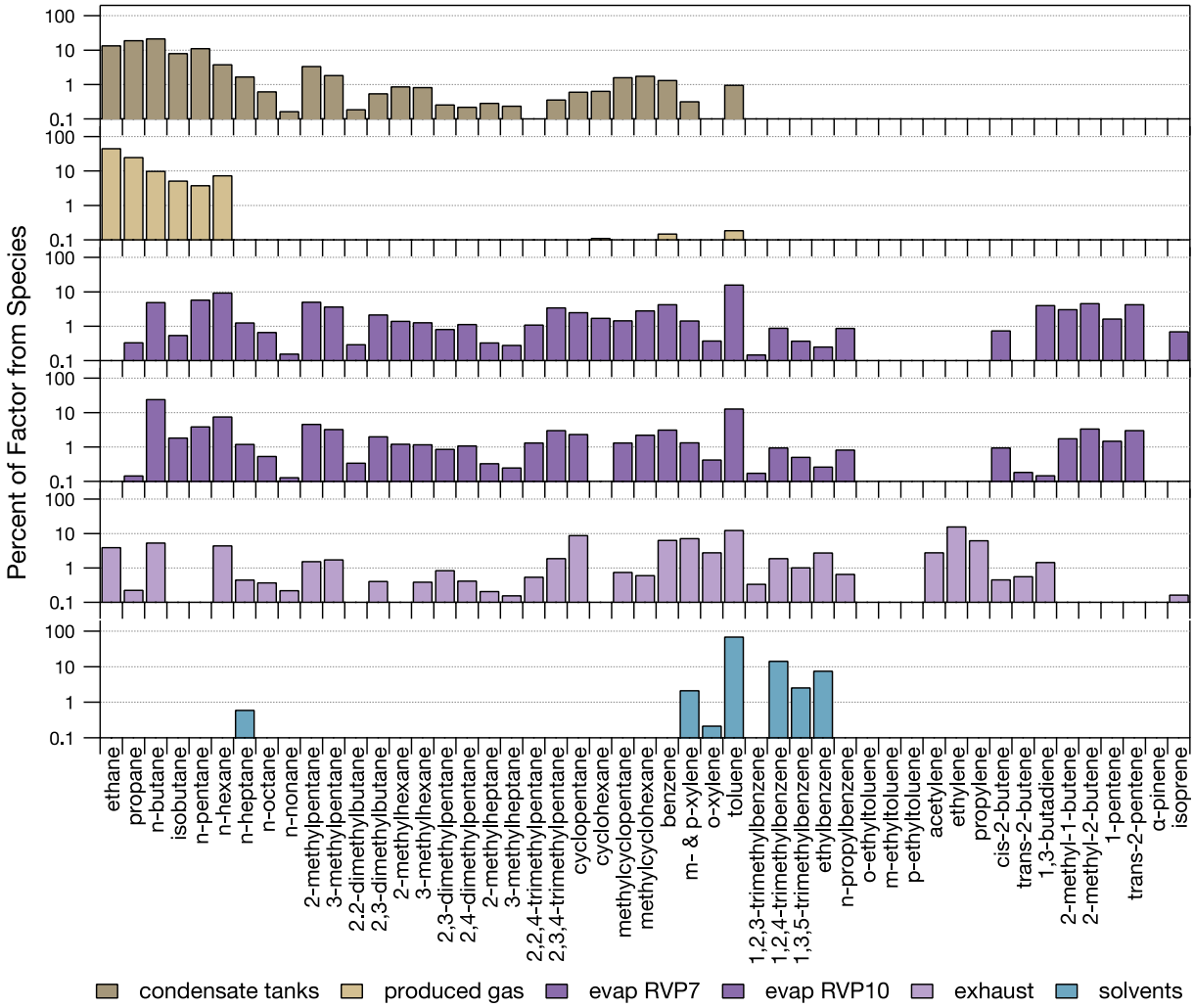

Fig. 2. Speciation profiles of each CMB source. Profiles of the percent of each NMHC species grouped by chemical family within which they are ordered by increasing carbon number by carbon (ppb C) in source profiles used with CMB. Note that the scale is logarithmic and that profiles for gasoline with two distinct Reid Vapor Pressures (RVP) are represented in the evaporative emissions in accordance with Table 1 but in the same color because they are a combined as a single source in the remainder of the figures. Profiles for sources consisting of a single species are not shown. (For interpretation of the references to color in this figure legend, the reader is referred to the Web version of this article.)

4. Results

4.1. CMB results

Numerous source profiles and combinations were run in CMB in order to arrive at the final list of source profiles (Table 1) used in the CMB calculations. After each CMB run the number of non-convergent runs and diagnostic statistics were examined in order to determine if the selected source profiles were appropriate. Fig. 2 shows the final set of profiles used in the CMB modeling. The source profiles for condensate tanks and produced gas, which constitute the O&NG sources, are dominated by straight chain alkanes though the profile for condensate tanks also includes more than 1% of some branched and cyclic alkanes as well as the toxic species benzene and toluene. The other anthropogenic source profiles (i.e., evaporative, exhaust, and solvents) each are constituted of more than 10% toluene. The evaporative emissions at either Reid Vapor Pressure have more branched alkenes than any other source profile though they also include straight chain, branched, and cyclic alkanes. The exhaust source profile is dominated by alkenes and BTEX compounds though some alkanes also contribute. Finally, solvents are almost entirely constituted of BTEX compounds.

With seven sources (represented by the five profiles shown in Fig. 2 plus isoprene and α-pinene), the CMB calculations resulted in 8 non-convergent samples out of 195 samples for Denver, and one non-convergent sample out of 177 samples for Platteville. The average percent mass accounted for, R^2, and χ^2 were 86%, 0.75, and 6.83, respectively for the Denver samples, and 88%, 0.83, and 6.13, respectively, for Platteville. For both locations, the average percent mass accounted for falls within the target range of 80%–120%. The average R^2 in Platteville is above the target of 0.8, but the Denver value is slightly below it. Although the average χ^2 at both locations exceeds the target of a maximum χ^2 of 4.0, the results shown correspond to the best fit of the attempted source selections. Results obtained with the addition of propane as a single-compound source did not improve the model performance so are not included here.

A time-series graph of the estimated mixing ratios by source (Fig. 3) provides insight into how each source contribution varies over time in Denver and Platteville. The condensate tanks and produced gas profiles dominate the source contributions at Platteville and are significantly smaller at Denver. Mixing ratios contributed by anthropogenic sources show winter peaks due to greater contributions from vehicles at cold temperatures and, perhaps, stronger temperature inversions that prevent pollutants from dispersing. The O&NG contributions decline somewhat over time in Platteville. As expected, the vehicle emissions profiles (i.e., exhaust and evaporative) have higher contributions in Denver than Platteville. The vehicle contributions appear to be relatively stable over the duration of the study. Biogenic contributions are not shown in Fig. 3 because they are generally low. As expected, they show pronounced seasonality with summer peaks.

4.2. PMF results

First, through exploratory analysis, the appropriate number of factors were selected for the unified data set. The number of factors, *p*, was varied from three to six using 100 runs for each *p*. Each solution was assessed for the degree to which the factors were consistent with a physically meaningful interpretation. The stability of the solution was characterized by the displacement technique, which quantifies rotational ambiguity or the dependence of the minimization of the correlation metric, *Q*, on the factor composition, by assessing the impact of slight adjustments to each factor on the value of the correlation metric, *Q*. Additionally, the stability of the solution was assessed with bootstrapping, which quantifies random errors and some effects of rotational ambiguity by determining the number of times that withholding a subset of the data would lead to misidentification, or swapping, of a factor resulting from factorization of the full dataset. The bootstrap analysis used 100 bootstrap runs with the default block size and a minimum correlation R-value of 0.6. In the exploratory analysis, the five-factor solution was most physically meaningful. It also had the greatest stability in the bootstrap runs with the factors swapping only 9 of 500 possible times, whereas the three-factor solution swapped 27 of 300 potential times, the four-factor solution swapped 40 out of 400 possible times, and the six-factor solution swapped 36 of 600 possible times. The displacement analysis showed that the three-, four-, and six-factor solutions had no sensitivity to displacement whereas the five-factor solution had a negligible decrease in the correlation metric, *Q*, with displacement but no swapping of factors.

Based on the results of the exploratory analysis, the five-factor solution, which was most stable, was selected for more comprehensive analysis. With the 100-run base solution and corresponding bootstrap and displacement error estimation in mind, the stability of the five-factor solution in rotational space was evaluated with F-peak analysis with F-peak values of [-1.0, −0.5, 0.5, 1.0]. The sum of the residuals increased less than 1% for each of the perturbations, which is well within the guidance that the run is acceptable if the increase is less than 5% of the robust sum of the residuals from the base run (Norris et al., 2014). The speciation profiles of the five factors as carbon fractions of the sum of NMHCs show the differentiation between factors in terms of contribution by each chemical family (Fig. 4), which can be compared against the CMB profiles (Fig. 2) (Section 4.3).

The apportionment of each compound to the five factors and the associated error estimates from the bootstrap technique help differentiate the sources with which the factors are likely to be associated (Fig. S8). The likely source, which is noted in the legend, was inferred from the key constituents of each factor and the time series of the contribution of each factor to the total NMHC mixing ratios (Fig. 5).

The chemical composition and temporal contribution of each factor supported its association with a source type. Unless otherwise noted, the statistics are drawn from the base case speciation profiles (Fig. S8). More than 40% by carbon mass of each of the C_6–C_9 straight alkanes are associated with the heavy oil and gas factor. Additionally, some of the larger branched or cyclic alkanes are more than 50% by carbon mass associated with this factor, including 2- and 3-methylheptane, and 80% by carbon mass of methylcyclohexane. Of note, 31% by carbon mass of benzene is associated with the heavy oil and gas factor. This factor might also be associated with diesel activity (Baldasano et al., 1998), which helps explain the relatively substantial contributions from this factor to observations in Denver. The annual contributions of this factor are 3–10 times higher in Platteville than in Denver without an identifiable temporal trend.

The light oil and gas factor contains more than 65% of the observed carbon mass of each of the C_2–C_4 straight alkanes as well as approximately 40% of the observed carbon mass of each of the C_6 branched alkanes. Associations of alkenes and ringed species with this factor are less than 20% by carbon mass. The annual contribution of this factor to observations at Denver are approximately 5–11% of those at Platteville with the smallest difference occurring in 2016 (Fig. 5), which may reflect declining contributions from the light oil and gas factor with time.

The traffic factor contains 74% and 55% of the observed carbon mass of acetylene and ethylene, respectively, which are indicative of traffic emissions (Bon et al., 2011; Gentner et al., 2013; Salameh et al., 2016). More than 40% by carbon mass of propylene (55%) and four branched alkenes are also associated with this factor. Between 20% and 40% of the BTEX and branched BTEX compounds are also associated with the traffic factor. This factor peaks in the winter months at similar levels for Denver and Platteville, though the annual contribution from this factor can be up to two times greater at the Denver site than at Platteville.

The urban factor represents approximately 40% by carbon mass of the BTEX and branched BTEX compounds and C_5 alkenes. More than 40% of the observed carbon mass of the branched C_8 alkanes are also

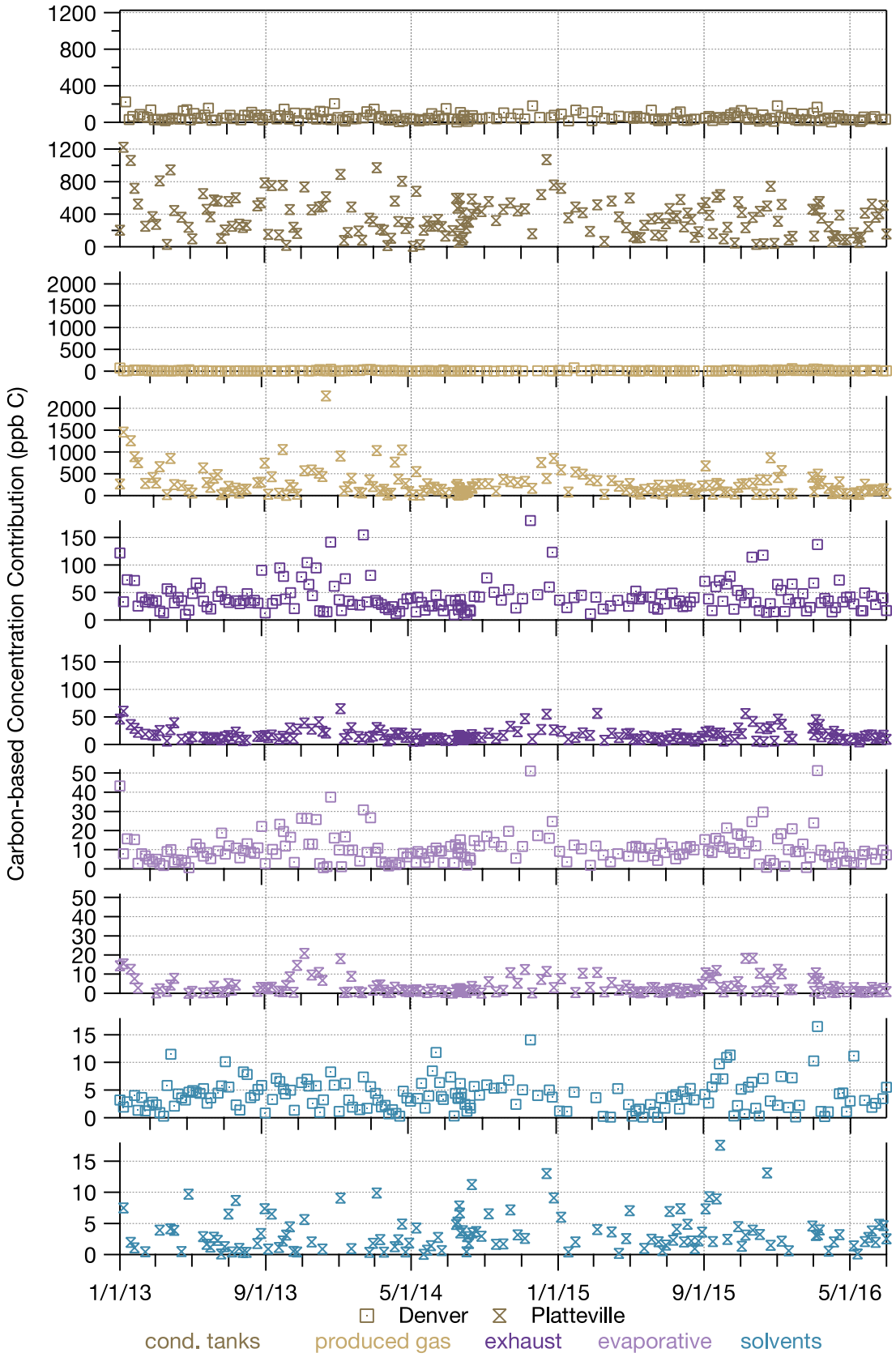

Fig. 3. CMB-based source contribution to each observation. Mixing ratio-based contribution (ppb C) of each CMB source at each observation. Observations made at the Denver (Platteville) site are indicated by squares (hourglass). Note the differing scales on the y-axes between each source, which are cutoff at zero even though some negative contributions result from the analysis.

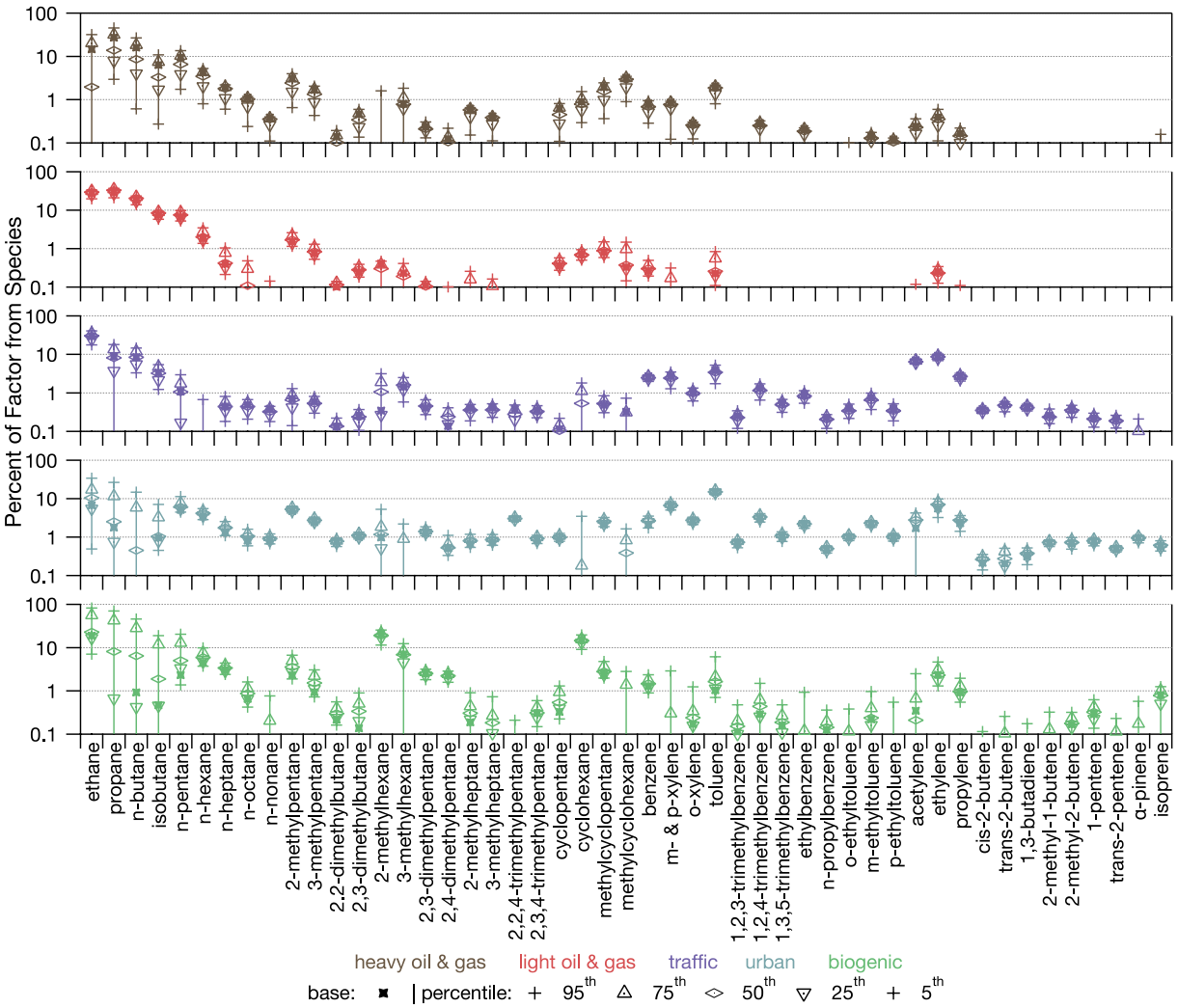

Fig. 4. PMF factors represented by the percent contribution of each species with variability. Profiles of each PMF factor by the percent contribution of each NMHC species by carbon (ppb C), which was determined from joint analysis of observations from Denver and Platteville, grouped by chemical family within which they are ordered by increasing carbon number. The sum across species for each factor is ~100%. The likely source associated with each factor is labeled in the legend, which is ordered with the sets of axes. The base symbol indicates the value that is used in the rest of the analysis for each species in each PMF factor. The percentiles reflect the variability of the factor solutions from the bootstrap runs. Note the logarithmic scale.

contained in this factor. Approximately 20% by carbon mass of the smaller alkenes are also associated with this factor. Included in this factor are also 63% and 40% by carbon mass of α-pinene and isoprene, respectively, which are emitted from vegetation (Guenther et al., 2006), yet these emissions are likely underestimated in these 6–9 am observations. Emissions of α-pinene and isoprene alongside other urban emissions cannot be expected to be entirely disentangled from other emissions types and, though likely a small fraction of the total emissions, isoprene has been observed in vehicular combustion emissions (Borbon et al., 2001; Reimann et al., 2000). The presence of BTEX compounds, branched BTEX compounds, C_5 alkenes, and branched C_8 alkanes in this factor indicate likely contributions from anthropogenic activity, perhaps including evaporative emissions, which differ from traffic emissions in that fuel is not combusted, and industrial activities, which may include chemical processing. Wildfires may have occasionally contributed to this factor, but no persistent influence was observed likely because of the intermittent nature of these events. The annual contributions of this factor are 3.5–7 times greater at Denver than at Platteville with slightly greater amounts in the fall and winter months than the spring and summer.

The factor labeled as biogenic contains 40% by carbon mass of isoprene, which is emitted from vegetation (Guenther et al., 2006). Greater than 30% by carbon mass of cyclohexane and larger branched alkanes are also associated with this factor. The peak contribution of this factor is typically in the summer, though the winter months from 2015 to 2016 consistently show a higher contribution. Since this factor's contribution changes with time, the annual contribution from it is greater in Platteville during the first two years but not during the last year and a half. The identification of this factor is uncertain due to the combination of compounds present, the seasonal timing, and the limitations of the OPS sampling and analysis protocol for biogenic compounds.

4.3. Comparison of CMB and PMF results

Comparing the carbon fraction CMB source profiles (Fig. 2) to the carbon fraction PMF factors (Fig. 4) reveals that the CMB condensate tanks profile is most similar to the PMF heavy and light oil and gas factor profiles, and the CMB vehicle exhaust profile is similar to the PMF traffic profile. The similarities are not complete, however. The PMF factor for heavy oil and gas compares well to the CMB tanks factor for alkanes and C_6 – C_8 aromatics, but the former includes higher fractions of trimethylbenzenes and alkenes than the CMB source profile. The presence of alkenes in this factor may be due to combustion sources that are

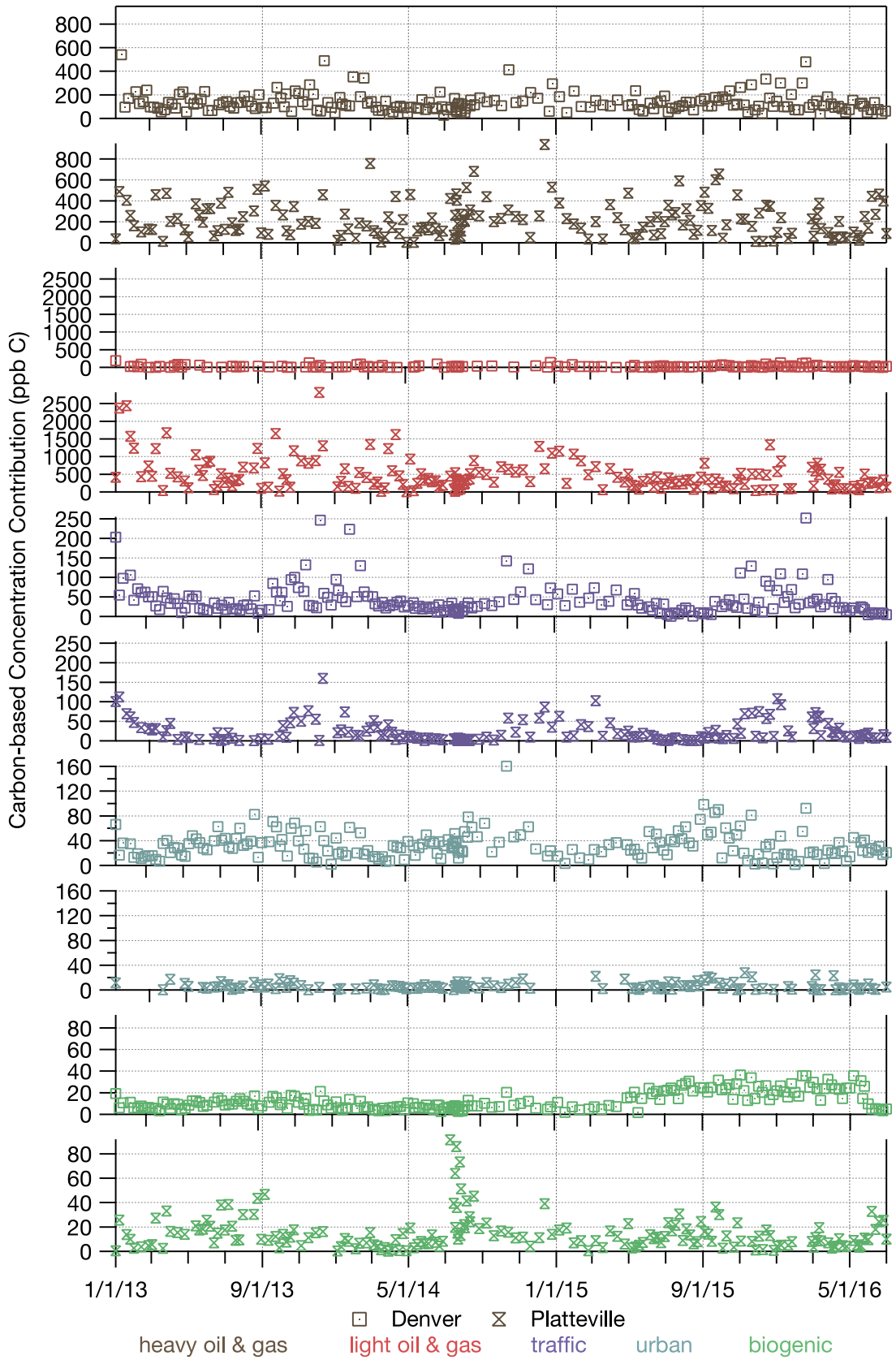

Fig. 5. PMF-based source contribution of each factor to each observation. Contributions are in terms of carbon (ppb C). Observations made at the Denver (Platteville) site are indicated by squares (hourglass). Note the differing scales on the y-axes between each factor. The source of which each factor is likely to be indicative is labeled in the legend, which is ordered with the pairs of axes.

associated or co-located with O&NG activities. The PMF factor identified as light oil and gas has more branched and cycloalkanes than the produced gas source profile used with CMB. The PMF traffic factor has significant carbon fractions for isobutane, n-pentane, and 2-methylhexane, which are not seen in the CMB vehicle exhaust profile. These discrepancies may be due to incompleteness of the CMB exhaust profile. Conversely, the CMB vehicle exhaust profile has higher carbon fractions of n-hexane, cyclohexane, and isoprene than are seen in the PMF traffic factor. The other profiles are more difficult to match between PMF and CMB. This is likely because PMF cannot clearly separate sources whose emissions are highly correlated, with factorization results reflecting correlations induced by chemical processing and meteorology as well as the sources of origin.

The observation-based factors extracted from the OPS data provide the opportunity to evaluate the emissions speciation profiles employed in CMB as well as those that are recommended for use in regional chemical transport modeling. Section S.6 presents a more detailed comparison of PMF factors with emissions speciation profiles from other studies, including profiles for emissions from condensate tanks, liquids load-out, and produced natural gas (Fig. S.9–10).

Figs. 3 and 5 show full time series of the CMB and PMF results, respectively. When comparing the CMB and PMF results, the magnitudes and time patterns of the corresponding source and factor are roughly similar. CMB estimates for condensate tanks are slightly higher than the PMF estimates for heavy oil and gas. The PMF light oil and gas estimates are slightly higher than the CMB produced gas estimates. The PMF traffic estimates are similar to the sum of the CMB vehicle exhaust and diurnal evaporative emissions estimates. However, there is a large difference between the two remaining categories. First, the urban PMF factor and the CMB solvent source differ in their relative contributions to each site, which is to be expected given that they represent different sources. Secondly, the biogenic factor contributes more significantly than the isoprene and α-pinene sources. The PMF biogenic factor estimates maximum mixing ratios of 80 ppb C, while the isoprene and α-pinene sources estimate a maximum mixing ratio of 3 and 2 ppb C, respectively. CMB treats isoprene and α-pinene as isolated biogenic species, whereas the PMF factor includes other species that are not biogenic in origin but are correlated with the biogenic compounds as sometimes occurs when the coincident concentrations and the number of factors are insufficient to differentiate biogenic influences completely (Kim et al., 2005; Sarkar et al., 2017).

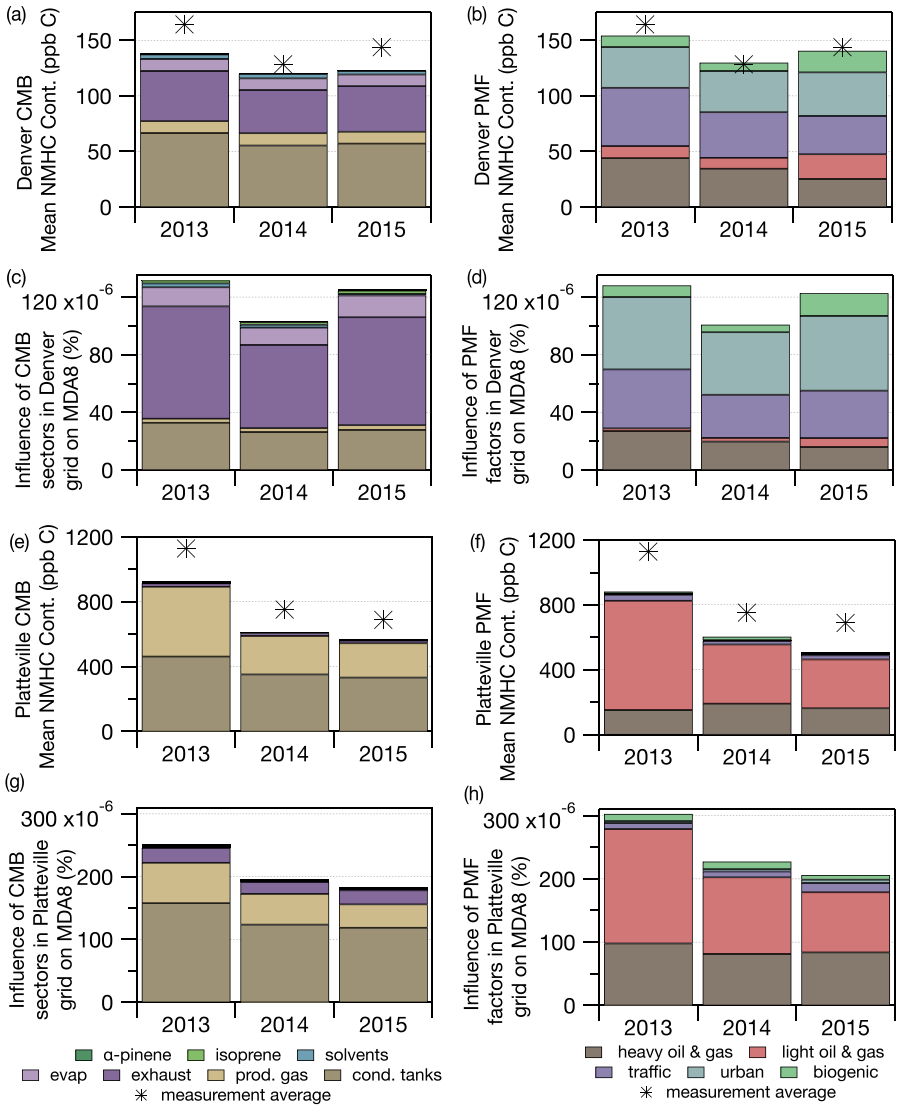

Fig. 6. Location-specific, CMB- and PMF-based contributions to NMHC and estimated MDA8 ozone. Annual average contributions to NMHC (ppb C) (rows 1 and 3) and MDA8 ozone in relative sense (%) (rows 2 and 4) for Denver (a–d) and Platteville (e–h) as estimated by CMB (left panel) and PMF (right panel).

4.4. Location-specific annual average contributions to NMHC, MDA8 ozone, and premature mortality with the CMAQ adjoint

Average source or factor contributions to 6–9 am NMHC mixing ratios at Denver and Platteville, respectively, were estimated with both CMB and PMF (Fig. 6a,b,e,f). For Denver (Platteville), the CMB model indicates that the sum of produced gas and condensate tanks contributes a yearly average of 63–77 (452–894) ppb C of NMHC with the contribution declining modestly from 2013 to 2015. The contribution estimated by PMF for the sum of the light and heavy O&NG factors ranges from 40.0 to 54.9 (384–837) ppb C of NMHC for Denver (Platteville). The sum of the vehicle exhaust and evaporative source contributions from CMB is relatively constant over time, averaging 40 (18) ppb C NMHC in Denver (Platteville). For comparison, the sum of vehicle exhaust and urban factor contributions from PMF is about 78 (35) ppb C NMHC in Denver (Platteville) and, again, is relatively constant over time.

To investigate ozone-related influences of emissions sources, location-specific sensitivities from the CMAQ adjoint are used to weight the results of the source apportionment models. Ozone impacts of the NMHCs are modulated by the abundance of both NMHCs and NOx. Typically, the potential ozone impact is estimated by using results from box modeling not specific to the local atmospheric conditions such as the maximum incremental reactivity scale (Carter, 2010) (e.g., Capps et al., 2010) or by calculating contributions to OH-reactivity (Gilman et al., 2013). Sensitivities that quantify the relationship of ozone metrics such as MDA8 and health impacts to location-specific emissions from the CMAQ adjoint are advantageous over these approaches. First, specific spatial and temporal metrics that are more relevant to policy or health outcomes can be quantified with the selection of a cost function for the adjoint than is possible with a generic box modeling approach. Additionally, the transport of emissions through space over time with variable ratios of NMHCs and NOx as well as light for photolysis is represented in the CMAQ adjoint. Representation of these processes is likely to lead to a more accurate estimate of the influence of NMHCs on ozone-related metrics that could not be quantified with the more typical approaches. Furthermore, this approach leverages empirical observations in a way that source apportionment conducted entirely within a modeling framework cannot; specifically, in this combined approach, the modeled emissions do not primarily dictate the relative influence of sources.

Relative contributions across sources or factors shift when adjoint weighting is used to estimate contributions to ozone instead of NMHC (Fig. 6c,d,g,h). The absence of coincident NOx measurements limits opportunities to consider the NOx influences observationally throughout this time frame, but the adjoint sensitivities of ozone with respect to NMHCs take into account the variations of modeled NOx levels in space and time. The modeled NOx-limited conditions across most of the Denver CSA with some conditions closer to VOC-limited in the urban core (Fig. S.11) are consistent with interpretations of observations during the FRAPPE and DISCOVER-AQ campaigns in the Front Range in 2014 (Pfister et al., 2017). The relative value of these location-specific contributions are very small because they represent a single 36 km × 36 km grid cell corresponding to either Denver or Platteville monitoring site, averaged over 3 h in the mornings. Also, the NMHCs include only the 49 species that were differentiated sufficiently for use in CMB and PMF, not total NMHCs; therefore, the relative influence estimates are smaller than those of total NMHC would be. Nevertheless, the temporal variation and relative source- or factor-specific contribution information provide useful insight for considering emissions control strategies.

Compared to their contributions to NMHC, O&NG sources or factors contribute a substantially smaller fraction to the adjoint-weighted mixing ratios for MDA8 ozone, while the shares estimated for vehicle emissions increase with adjoint-weighting. The CMB results indicate that between 2013 and 2015 vehicle exhaust and evaporative emissions accounted for an average of 69% (11%) of the MDA8 ozone contribution in Denver (Platteville), even though it accounts for only 41% (3%) of the NMHC contribution. The reactivity of NMHCs emitted in this process is likely the primary reason traffic has an increased contribution to ozone formation than the carbon-based fraction, but the simultaneous emission of NOx with vehicle exhaust may also contribute to the increased effectiveness of this source. In contrast, condensate tanks and produced gas accounted for an estimated 56% of the NMHC contribution in Denver but only for 27% of the MDA8 ozone contribution, whereas these sources account for an estimated 96% of the NMHC versus 88% of MDA8 ozone in Platteville. The PMF results indicate that while traffic and urban emissions in Denver (Platteville) represented 53% (8%) of the NMHC contribution, an estimated 71% (6%) of the MDA8 ozone contribution is due to traffic and urban factors. In contrast, the heavy and light oil and gas factors account for 33% of the NMHC contribution in Denver but only for 21% of the MDA8 ozone contribution, whereas these account for an estimated 92% of the NMHC and 89% of MDA8 ozone in Platteville.

The percentage contributions of CMB sources and PMF factors to ozone-related premature mortality (Fig. 7) are similar to those for MDA8 ozone with minimal differences arising from different averaging times, population weighting, and the MDA8 cutoff value, TMREL, introduced by the ozone concentration metric in the exposure-response model (Lyu et al., 2019). However, it is worth noting that NMHC mixing ratios in the Platteville grid cell contribute more to the MDA8 and premature mortality in the Denver CSA than those in the Denver grid cell, mainly because of the absolutely higher NMHC levels in the Platteville grid cell despite lower ozone sensitivities (Fig. 6). The implication of this finding is that the emissions of NMHC from O&NG activities near Platteville are crucial to public health in the populous Denver CSA.

4.5. Contributions to benzene and toluene

Fig. 8 shows annual average CMB and PMF-estimated contributions to benzene and toluene in Denver and Platteville, respectively. More detailed results including estimates of variability are shown in Figures S.12-19. For both locations, CMB overestimates benzene mixing ratios and generally overestimates toluene mixing ratios. It appears that the benzene fractions are too high in both the vehicle and O&NG source profiles used with CMB. On an annual average basis, total factor contributions from PMF match the measured mixing ratios relatively well. The CMB analysis suggests that vehicle emissions are the major source of benzene and toluene in Denver. The PMF model suggests the traffic factor is the major source of benzene in Denver (Fig. S.20), while the urban factor is the major source of toluene. For Platteville, CMB suggests that condensate tanks are the largest source of benzene, with vehicle exhaust and solvent evaporation also contributing significant toluene. PMF suggests the oil and gas-identified factors are the main sources of both benzene and toluene for the Platteville site. These results are consistent with the correlations of benzene with acetylene, a marker of traffic emissions, being stronger in Denver than with propane, an indicator of O&NG emissions, in 2013; the converse was true in Platteville (Thompson et al., 2014).

4.6. Comparison of contributions with previous work

Results from this study show some contrasts with prior work conducted in the DJ Basin, but they may be explained by differences in study locations and timing. For example, Thompson et al. (2014) found that mean mixing ratios of n-butane and benzene in east Boulder County increased by factors of two and three, respectively, between 2007 and 2013. In contrast, the CDPHE data for benzene at Denver and Platteville indicate that average mixing ratios were lower in 2014 and 2015 than 2013 (p values < 0.05 for one-sided student's t-test). Average mixing ratios of n-butane at the CDPHE site in Platteville were lower by a factor of about 1.8 in January through June of 2016 than in the same months of

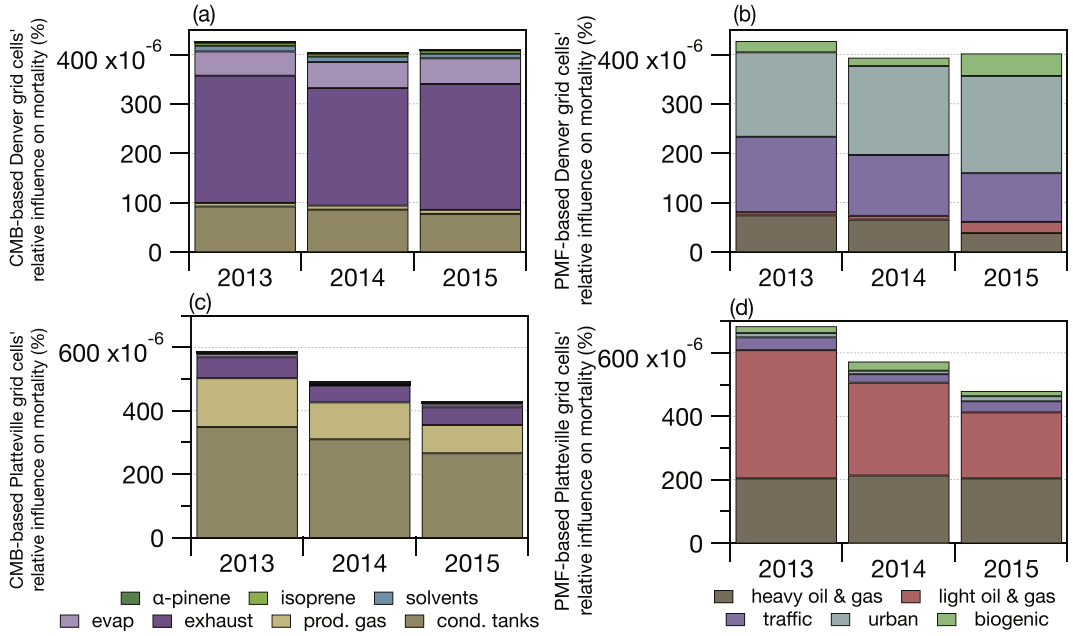

Fig. 7. Location-specific, CMB- and PMF-based annual average relative contributions to ozone-related premature mortality in the Denver CSA for 6–9 am mixing ratios from Denver (a–b) and Platteville (c–d) grid cells as estimated by CMB (left panel) and PMF (right panel).

2013. Additionally, average mixing ratios of n-butane at the CDPHE site in Platteville in 2014 and 2015 were lower than those in 2013 ($p < 0.05$). In contrast to the earlier time period when O&NG emissions were suggested to be increasing throughout the Denver-Julesburg basin by Thompson et al. (2014), the imposition of controls and/or improved operating practices may have led to reduced emissions over the 2013 to 2016 time period, at least nearby the Platteville monitoring site.

The early study by Pétron et al. (2012) with data from 2007 to 2010 found measured alkane ratios from their mobile laboratory and the BAO tower to be in good agreement with emissions profiles for condensate tank flash emissions and oil and gas venting. This study similarly finds flash emissions and leaks or venting to be important sources of alkanes, especially at the Platteville site (Section S.5, Fig. S.9-10). Based on measurements at the BAO tower in winter 2011, Gilman et al. (2013) estimated that O&NG emissions contributed 70% or more of the observed $C_2 - C_7$ alkanes, 20–30% of benzene, toluene, and xylenes, and an average of 55% of the OH-reactivity of the NMHC mixture. By applying PMF to measurements made at the BAO tower in spring and summer 2015, Abeleira et al. (2017) estimated that O&NG emissions contributed 36–100% of $C_2 - C_6$ alkanes, 70% of benzene, 30–40% of toluene, and 40–70% of the OH-reactivity of VOCs. Using PMF and CMB with an adjoint-weighted scheme rather than OH-reactivity weighting, we find that adjoint-based contribution to MDA8 from O&NG is 21–27% in Denver and about 88% in Platteville. The adjoint-based contributions to premature mortality are very close to those of MDA8 because of the similar formulation of these metrics. Adjoint sensitivities could be refined in future work by updating the base year and emissions inventory used in the adjoint modeling and mortality analyses, and by updating the chemical mechanism. The O&NG contributions we estimated for alkanes, benzene, and toluene from CDPHE measurements at Denver are generally lower, and those for Platteville higher, than the contributions estimated from the BAO tower measurements. This is expected, since the tower is situated between Denver and Platteville and on the western edge of the DJ Basin rather than in the heart of it.

Based on data from spring 2012, Pétron et al. (2014) found that O&NG emissions of benzene in Weld County might be equal to or greater than mobile source contributions. Our average estimates for 2013–2015 from CMB and PMF suggest that O&NG emissions account for most of the benzene at CDPHE's Platteville monitoring site. This result agrees with Halliday et al. (2016) findings for benzene based on data collected at a site 9 km southeast of Platteville in summer 2014.

5. Conclusions

This study complements other source apportionment studies for northeastern Colorado by analyzing NMHC data from two contrasting measurement sites – a site in Platteville and one in Denver, and by taking advantage of the 2013–2016 time period for ongoing data collection, which coincides with the implementation of new O&NG control requirements and operating practices. In contrast, previous studies have covered either older or shorter sampling periods and focused on data from the DJ Basin or the BAO tower, which is located on the edge of the Basin. In this study the PMF and CMB models are complementary, enabling us to examine whether statistically derived factors match profiles for known sources, and in turn to identify where published source profiles may not fully represent sources in the North Front Range. The results from both models showed reasonable agreement for the O&NG and vehicle profiles/factors.

A limitation of all source apportionment studies, including this one, is that their statistically derived results are only representative of emissions influencing the measurement location or locations, and the time periods covered by the data. In particular for this study, the results represent source apportionment estimates for the 6 am–9 am sampling period used in CDPHE's ozone precursor study. This time period is advantageous for sampling anthropogenic NMHC from nearby sources because it typically corresponds to the highest mixing ratios of the day, due to shallow mixing depths, light winds, and limited time for photochemical processing. On the other hand, biogenic emissions are likely underrepresented during this time period. Additionally, at Denver and Platteville, winds during this time of day are relatively light and variable (Toth and Johnson, 1985), so the morning sampling period may miss larger influences from O&NG emissions that impact the monitoring sites in association with stronger northeasterly winds.

As shown in Table 1, the average mixing ratios of total NMHC at CDPHE's Platteville monitoring site were higher in 2013 than in the next two and a half years. The CMB model results suggest that the lower NMHC mixing ratios at this particular location may be attributable to both lower production emissions and lower flash emissions (Fig. 7e),

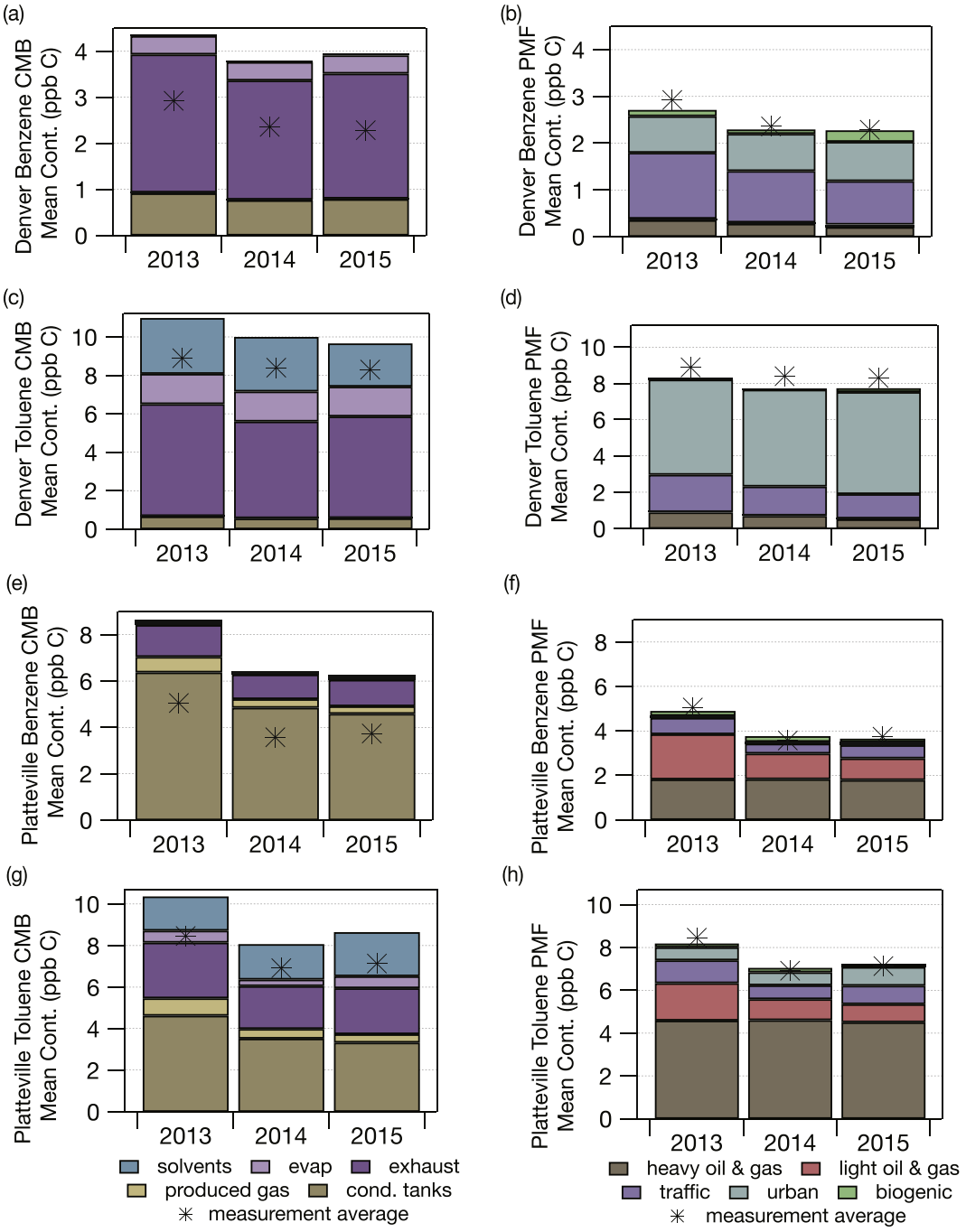

Fig. 8. Location-specific, CMB- and PMF-based contributions to benzene and toluene. Annual average contributions to benzene (rows 1 and 3) and toluene (rows 2 and 4) (ppb C) for Denver (a–d) and Platteville (e–h) as estimated by CMB (left panel) and PMF (right panel).

whereas the PMF results attribute the change to reductions in light oil and gas emissions (Fig. 7f). Either way, new regulations implemented by the state as well as changes in operating practices made by the industry for other reasons might explain the observation that NMHC mixing ratios at the Platteville site were lower in 2016 than in 2013. In contrast to the O&NG contributions at the Platteville site, total NMHC mixing ratios in Denver and, in particular, the vehicle emissions contributions there show little change over the study time period. Continued NMHC measurements and measurements at more locations are needed to ascertain whether recently adopted O&NG regulations are having their intended effect. The adjoint-based analysis suggests that O&NG-related NMHCs near the Platteville site contribute to at least as much ozone-related premature mortality in the Denver CSA as vehicular NMHCs adjacent to the Denver site. Likewise, PMF and CMB indicate that the largest contributions to benzene in Platteville are from O&NG and that these are larger than the contributions of traffic-related emissions, which is the largest relative contributor, to Denver concentrations. Therefore, further attention to vehicle emissions as well as O&NG emissions appears warranted, as the Denver and North Front Range area continues its efforts to improve air quality.

CRediT authorship contribution statement

Congmeng Lyu: Formal analysis, Investigation, Data curation, Writing - original draft, preparation, Visualization. **Shannon L. Capps:** Conceptualization, Methodology, Software, Formal analysis,

Investigation, Data curation, Writing - original draft, Writing - review & editing, Visualization, Supervision, Project administration. **Kent Kurashima:** Formal analysis, Investigation, Data curation, Writing - original draft, Visualization. **Daven K. Henze:** Software, Writing - review & editing, Supervision. **Gordon Pierce:** Validation, Resources, Data curation, Writing - review & editing. **Amir Hakami:** Software. **Shunliu Zhao:** Software. **Jaroslav Resler:** Software. **Gregory R. Carmichael:** Software. **Adrian Sandu:** Software. **Armistead G. Russell:** Software. **Tianfeng Chai:** Software. **Jana Milford:** Conceptualization, Validation, Formal analysis, Resources, Writing - original draft, Writing - review & editing, Supervision, Project administration, Funding acquisition.

Declaration of competing interest

The authors declare that they have no known competing financial interests or personal relationships that could have appeared to influence the work reported in this paper.

Acknowledgments, Samples, and Data

This research was supported in part by the AirWaterGas Sustainability Research Network funded by the National Science Foundation under Grant No. CBET-1240584. Any opinions, findings, and conclusions or recommendations expressed in this paper are those of the author and do not necessarily reflect the views of the National Science Foundation. The authors have declared that no competing interests exist. The CDPHE North Front Range Ozone Precursor Monitoring data are available at https://www.colorado.gov/airquality/tech_doc_repository.aspx. The CMAQ adjoint model and inputs are available upon request from the corresponding author.

Appendix A. Supplementary data

Supplementary data to this article can be found online at https://doi.org/10.1016/j.atmosenv.2020.118113.

References

Abeleira, A., Pollack, I.B., Sive, B., Zhou, Y., Fischer, E.V., Farmer, D.K., 2017. Source characterization of volatile organic compounds in the Colorado Northern Front Range Metropolitan Area during spring and summer 2015. J. Geophys. Res.: Atmosphere 122, 3595–3613.

Air Pollution Control Division, 2017. 2016 Colorado Air Quality Data Report. Colorado Department of Public Health and the Environment, Denver, Colorado.

Baldasano, J.M., Delgado, R., Calbó, J., 1998. Applying receptor models to analyze urban/suburban VOCs air quality in martorell (Spain). Environ. Sci. Technol. 32, 405–412.

Bon, D.M., Ulbrich, I.M., de Gouw, J.A., Warneke, C., Kuster, W.C., Alexander, M.L., Baker, A., Beyersdorf, A.J., Blake, D., Fall, R., Jimenez, J.L., Herndon, S.C., Huey, L. G., Knighton, W.B., Ortega, J., Springston, S., Vargas, O., 2011. Measurements of volatile organic compounds at a suburban ground site (T1) in Mexico City during the MILAGRO 2006 campaign: measurement comparison, emission ratios, and source attribution. Atmos. Chem. Phys. 11, 2399–2421.

Borbon, A., Fontaine, H., Veillerot, M., Locoge, N., Galloo, J.C., Guillermo, R., 2001. An investigation into the traffic-related fraction of isoprene at an urban location. Atmos. Environ. 35, 3749–3760.

Brantley, H.L., Thoma, E.D., Eisele, A.P., 2015. Assessment of volatile organic compound and hazardous air pollutant emissions from oil and natural gas well pads using mobile remote and on-site direct measurements. J. Air Waste Manag. Assoc. 65, 1072–1082, 1995.

Brown, S.G., Frankel, A., Hafner, H.R., 2007. Source apportionment of VOCs in the Los Angeles area using positive matrix factorization. Atmos. Environ. 41, 227–237.

Capps, S.L., Hu, Y.T., Russell, A.G., 2010. Assessing near-field and downwind impacts of reactivity-based substitutions. J. Air Waste Manag. Assoc. 60, 316–327.

Carter, W.P.L., 2010. Updated Maximum Incremental Reactivity Scale and Hydrocarbon Bin Reactivities for Regulatory Applications. University of California, Riverside, CA.

CDPHE, 2017. Control of Ozone Precursors and Control of Hydrocarbons via Oil and Gas Emissions. Colorado Department of Public Health and the Environment, Denver, Colorado.

CDPHE, 2018. Standard Operating Procedure for the Determination of Toxic Organic Compounds in Ambient Air. Appendix GM13. Colorado Department of Public Health and Environment, Air Pollution Control Division, Denver, Colorado available upon request.

COGCC, 2017. COGIS production data inquiry. Colorado Oil and Gas Conservation Commission. https://cogcc.state.co.us/cogis/ProductionSearch.asp.

Cohen, A.J., Brauer, M., Burnett, R., Anderson, H.R., Frostad, J., Estep, K., Balakrishnan, K., Brunekreef, B., Dandona, L., Dandona, R., Feigin, V., Freedman, G., Hubbell, B., Jobling, A., Kan, H., Knibbs, L., Liu, Y., Martin, R., Morawska, L., Pope, C.A., Shin, H., Straif, K., Shaddick, G., Thomas, M., van Dingenen, R., van Donkelaar, A., Vos, T., Murray, C.J.L., Forouzanfar, M.H., 2017. Estimates and 25-year trends of the global burden of disease attributable to ambient air pollution: an analysis of data from the Global Burden of Diseases Study 2015. Lancet 389, 1907–1918.

Coulter, T., 2004. EPA-CMB8.2 Users Manual. U.S. Environmental Protection Agency, Research Triangle Park, NC.

ERG, 2015. Support for the EPA National Monitoring Programs, Contract No. EP-D-14-030, Quality Assurance Project Plan. Eastern Research Group, Inc., Morrisville, North Carolina available upon request.

ERG, 2016. Standard Operating Procedure for Sample Canister Cleaning Using the Wasson TO-Clean Automated System, ERG-MOR-105 M, Morrisville. North Carolina available upon request.

Flocke, F., Pfister, G., Crawford, J.H., Pickering, K.E., Pierce, G., Bon, D., Reddy, P., 2020. Air quality in the northern Colorado Front range Metro area: the Front range air pollution and photochemistry Éxperiment (FRAPPÉ). J. Geophys. Res.: Atmosphere 125.

Fujita, E.M., Watson, J.G., Chow, J.C., Magliano, K.L., 1995. Receptor model and emissions inventory source apportionments of nonmethane organic gases in California's San Joaquin valley and San Francisco bay area. Atmos. Environ. 29, 3019–3035.

Gentner, D.R., Worton, D.R., Isaacman, G., Davis, L.C., Dallmann, T.R., Wood, E.C., Herndon, S.C., Goldstein, A.H., Harley, R.A., 2013. Chemical composition of gas-phase organic carbon emissions from motor vehicles and implications for ozone production. Environ. Sci. Technol. 47, 11837–11848.

Gilman, J.B., Lerner, B.M., Kuster, W.C., de Gouw, J.A., 2013. Source signature of volatile organic compounds from oil and natural gas operations in northeastern Colorado. Environ. Sci. Technol. 47, 1297–1305.

Guenther, A., Karl, T., Harley, P., Wiedinmyer, C., Palmer, P.I., Geron, C., 2006. Estimates of global terrestrial isoprene emissions using MEGAN (model of emissions of gases and aerosols from nature). Atmos. Chem. Phys. 6, 3181–3210.

Hakami, A., Henze, D.K., Seinfeld, J.H., Singh, K., Sandu, A., Kim, S., Byun, D., Li, Q., 2007. The adjoint of CMAQ. Environ. Sci. Technol. 41, 7807–7817.

Halliday, H.S., Thompson, A.M., Wisthaler, A., Blake, D.R., Hornbrook, R.S., Mikoviny, T., Müller, M., Eichler, P., Apel, E.C., Hills, A.J., 2016. Atmospheric benzene observations from oil and gas production in the denver-Julesburg basin in july and August 2014. J. Geophys. Res.: Atmosphere 121 (11), 055-011,074.

Harley, R.A., Hannigan, M.P., Cass, G.R., 1992. Respeciation of organic gas emissions and the detection of excess unburned gasoline in the atmosphere. Environ. Sci. Technol. 26, 2395–2408.

Hasheminassab, S., Daher, N., Saffari, A., Wang, D., Ostro, B.D., Sioutas, C., 2014. Spatial and temporal variability of sources of ambient fine particulate matter (PM2.5) in California. Atmos. Chem. Phys. 14, 12085–12097.

Haskew, H., 2010. Evaporative Emissions from In-Use Vehicles: Test Fleet Expansion (CRC E-77-2b) Final Report.

Jorquera, H., Rappenglück, B., 2004. Receptor modeling of ambient VOC at Santiago, Chile. Atmos. Environ. 38, 4243–4263.

Kelly, T.J., Holdren, M.W., 1995. Applicability of canisters for sample storage in the determination of hazardous air pollutants. Atmos. Environ. 29, 2595–2608.

Kim, E., Brown, S.G., Hafner, H.R., Hopke, P.K., 2005. Characterization of non-methane volatile organic compounds sources in Houston during 2001 using positive matrix factorization. Atmos. Environ. 39, 5934–5946.

Kim, E., Hopke, P.K., 2004. Improving source identification of fine particles in a rural northeastern U.S. area utilizing temperature-resolved carbon fractions. J. Geophys. Res.: Atmosphere 1984–2012, 109.

Kim, E., Hopke, P.K., 2008. Source characterization of ambient fine particles at multiple sites in the Seattle area. Atmos. Environ. 42, 6047–6056.

Kurashima, K., 2018. Mechanical Engineering Graduate Theses & Dissertations. Low Cost Air Quality and Sound Level Meters in Denver Schools and Source Apportionment of Volatile Organic Compounds with the Chemical Mass Balance Model, vol. 165. University of Colorado, Boulder, CO.

Leuchner, M., Rappenglück, B., 2010. VOC source–receptor relationships in Houston during TexAQS-II. Atmos. Environ. 44, 4056–4067.

Liang, C.-K., West, J.J., Silva, R.A., Bian, H., Chin, M., Davila, Y., Dentener, F.J., Emmons, L., Flemming, J., Folberth, G., Henze, D., Im, U., Jonson, J.E., Keating, T.J., Kucsera, T., Lenzen, A., Lin, M., Lund, M.T., Pan, X., Park, R.J., Pierce, R.B., Sekiya, T., Sudo, K., Takemura, T., 2018. HTAP2 multi-model estimates of premature human mortality due to intercontinental transport of air pollution and emission sectors. Atmos. Chem. Phys. 18, 10497–10520.

Lim, S.S., Vos, T., Flaxman, A.D., Danaei, G., Shibuya, K., Adair-Rohani, H., AlMazroa, M. A., Amann, M., Anderson, H.R., Andrews, K.G., Aryee, M., Atkinson, C., Bacchus, L. J., Bahalim, A.N., Balakrishnan, K., Balmes, J., Barker-Collo, S., Baxter, A., Bell, M. L., Blore, J.D., Blyth, F., Bonner, C., Borges, G., Bourne, R., Boussinesq, M., Brauer, M., Brooks, P., Bruce, N.G., Brunekreef, B., Bryan-Hancock, C., Bucello, C., Buchbinder, R., Bull, F., Burnett, R.T., Byers, T.E., Calabria, B., Carapetis, J., Carnahan, E., Chafe, Z., Charlson, F., Chen, H., Chen, J.S., Cheng, A.T.-A., Child, J. C., Cohen, A., Colson, K.E., Cowie, B.C., Darby, S., Darling, S., Davis, A., Degenhardt, L., Dentener, F., Des Jarlais, D.C., Devries, K., Dherani, M., Ding, E.L., Dorsey, E.R., Driscoll, T., Edmond, K., Ali, S.E., Engell, R.E., Erwin, P.J., Fahimi, S., Falder, G., Farzadfar, F., Ferrari, A., Finucane, M.M., Flaxman, S., Fowkes, F.G.R., Freedman, G., Freeman, M.K., Gakidou, E., Ghosh, S., Giovannucci, E., Gmel, G.,

Graham, K., Grainger, R., Grant, B., Gunnell, D., Gutierrez, H.R., Hall, W., Hoek, H. W., Hogan, A., Hosgood, H.D., Hoy, D., Hu, H., Hubbell, B.J., Hutchings, S.J., Ibeanusi, S.E., Jacklyn, G.L., Jasrasaria, R., Jonas, J.B., Kan, H., Kanis, J.A., Kassebaum, N., Kawakami, N., Khang, Y.-H., Khatibzadeh, S., Khoo, J.-P., Kok, C., Laden, F., Lalloo, R., Lan, Q., Lathlean, T., Leasher, J.L., Leigh, J., Li, Y., Lin, J.K., Lipshultz, S.E., London, S., Lozano, R., Lu, Y., Mak, J., Malekzadeh, R., Mallinger, L., Marcenes, W., March, L., Marks, R., Martin, R., McGale, P., McGrath, J., Mehta, S., Memish, Z.A., Mensah, G.A., Merriman, T.R., Micha, R., Michaud, C., Mishra, V., Hanafiah, K.M., Mokdad, A.A., Morawska, L., Mozaffarian, D., Murphy, T., Naghavi, M., Neal, B., Nelson, P.K., Nolla, J.M., Norman, R., Olives, C., Omer, S.B., Orchard, J., Osborne, R., Ostro, B., Page, A., Pandey, K.D., Parry, C.D.H., Passmore, E., Patra, J., Pearce, N., Pelizzari, P.M., Petzold, M., Phillips, M.R., Pope, D., Pope, C.A., Powles, J., Rao, M., Razavi, H., Rehfuess, E.A., Rehm, J.T., Ritz, B., Rivara, F.P., Roberts, T., Robinson, C., Rodriguez-Portales, J.A., Romieu, I., Room, R., Rosenfeld, L.C., Roy, A., Rushton, L., Salomon, J.A., Sampson, U., Sanchez-Riera, L., Sanman, E., Sapkota, A., Seedat, S., Shi, P., Shield, K., Shivakoti, R., Singh, G.M., Sleet, D.A., Smith, E., Smith, K.R., Stapelberg, N.J.C., Steenland, K., Stöckl, H., Stovner, L.J., Straif, K., Straney, L., Thurston, G.D., Tran, J. H., Van Dingenen, R., van Donkelaar, A., Veerman, J.L., Vijayakumar, L., Weintraub, R., Weissman, M.M., White, R.A., Whiteford, H., Wiersma, S.T., Wilkinson, J.D., Williams, H.C., Williams, W., Wilson, N., Woolf, A.D., Yip, P., Zielinski, J.M., Lopez, A.D., Murray, C.J.L., Ezzati, M., 2014. A comparative risk assessment of burden of disease and injury attributable to 67 risk factors and risk factor clusters in 21 regions, 1990–2010: a systematic analysis for the Global Burden of Disease Study 2010. Lancet 380, 2224–2260.

Lyu, C., Capps, S.L., Hakami, A., Zhao, S., Resler, J., Carmichael, G.R., Sandu, A., Russell, A.G., Chai, T., Henze, D.K., 2019. Elucidating emissions control strategies for ozone to protect human health and public welfare within the continental United States. Environ. Res. Lett. 14, 124093.

Malley, C.S., Henze, D.K., Kuylenstierna, J.C.I., Vallack, H.W., Davila, Y., Anenberg, S.C., Turner, M.C., Ashmore, M.R., 2017. Updated global estimates of respiratory mortality in adults >/=30Years of age attributable to long-term ozone exposure. Environ. Health Perspect. 125, 087021.

McDuffie, E.E., Edwards, P.M., Gilman, J.B., Lerner, B.M., Dubé, W.P., Trainer, M., Wolfe, D.E., Angevine, W.M., deGouw, J., Williams, E.J., Tevlin, A.G., Murphy, J.G., Fischer, E.V., McKeen, S., Ryerson, T.B., Peischl, J., Holloway, J.S., Aikin, K., Langford, A.O., Senff, C.J., Alvarez, R.J., Hall, S.R., Ullmann, K., Lantz, K.O., Brown, S.S., 2016. Influence of oil and gas emissions on summertime ozone in the Colorado Northern Front Range. J. Geophys. Res.: Atmosphere 121, 8712–8729.

McKenzie, L.M., Blair, B., Hughes, J., Allshouse, W.B., Blake, N.J., Helmig, D., Milmoe, P., Halliday, H., Blake, D.R., Adgate, J.L., 2018. Ambient nonmethane hydrocarbon levels along Colorado's northern Front range: acute and chronic health risks. Environ. Sci. Technol. 52, 4514–4525.

Milford, J.B., 2014. Out in Front? State and federal regulation of air pollution emissions from oil and gas production activities in the western United States. Nat. Resour. J. 55, 1–45.

Norris, G.A., Duvall, R., Brown, S.G., Bai, S., 2014. EPA Positive Matrix Factorization (PMF) 5.0 Fundamentals and User Guide.

Paatero, P., Tapper, U., 1994. Positive matrix factorization: a non negative factor model with optimal utilization of error estimates of data values. Environmetrics 5, 111–126.

Pétron, G., Frost, G., Miller, B.R., Hirsch, A.I., Montzka, S.A., Karion, A., Trainer, M., Sweeney, C., Andrews, A.E., Miller, L., Kofler, J., Bar-Ilan, A., Dlugokencky, E.J., Patrick, L., Moore, C.T., Ryerson, T.B., Siso, C., Kolodzey, W., Lang, P.M., Conway, T., Novelli, P., Masarie, K., Hall, B., Guenther, D., Kitzis, D., Miller, J., Welsh, D., Wolfe, D., Neff, W., Tans, P., 2012. Hydrocarbon emissions characterization in the Colorado Front Range: a pilot study. J. Geophys. Res.: Atmosphere 1984–2012, 117.

Pétron, G., Karion, A., Sweeney, C., Miller, B.R., Montzka, S.A., Frost, G.J., Trainer, M., Tans, P., Andrews, A., Kofler, J., Helmig, D., Guenther, D., Dlugokencky, E., Lang, P., Newberger, T., Wolter, S., Hall, B., Novelli, P., Brewer, A., Conley, S., Hardesty, M., Banta, R., White, A., Noone, D., Wolfe, D., Schnell, R., 2014. A new look at methane and nonmethane hydrocarbon emissions from oil and natural gas operations in the Colorado Denver-Julesburg Basin. J. Geophys. Res.: Atmosphere 119, 6836–6852.

Pfister, G.G., Flocke, F., Hornbrook, R.S., Orlando, J., Lee, S., 2017. Process-Based and Regional Source Impact Analysis for FRAPPE and DISCOVER-AQ 2014, *Final Report To the Colorado Department Of Public Health And the Environment*. National Center for Atmospheric Research, Boulder, CO.

Polissar, A.V., Hopke, P.K., Paatero, P., Malm, W.C., Sisler, J.F., 1998. Atmospheric aerosol over Alaska: 2. Elemental composition and sources. J. Geophys. Res.: Atmosphere 103, 19045–19057.

Rao, V., Tooly, L., Drukenbrod, J., Agency, E.P., 2013. 2008 National Emissions Inventory: Review, Analysis and Highlights, p. 78p.

Regional Air Quality Council, 2016. Moderate Area 2008 8-Hour Ozone Standard State Implementation Plan. Denver, Colorado.

Reimann, S., Calanca, P., Hofer, P., 2000. The anthropogenic contribution to isoprene concentrations in a rural atmosphere. Atmos. Environ. 34, 109–115.

Salameh, T., Sauvage, S., Afif, C., Borbon, A., Locoge, N., 2016. Source apportionment vs. emission inventories of non-methane hydrocarbons (NMHC) in an urban area of the Middle East: local and global perspectives. Atmos. Chem. Phys. 16, 3595–3607.

Sandu, A., Sander, R., 2005. KPP-2.1 User's Manual, pp. 1–29.

Sarkar, C., Sinha, V., Sinha, B., Panday, A.K., Rupakheti, M., Lawrence, M.G., 2017. Source apportionment of NMVOCs in the Kathmandu Valley during the SusKat-ABC international field campaign using positive matrix factorization. Atmos. Chem. Phys. 17, 8129–8156.

Scheff, P.A., Wadden, R.A., 1993. Receptor modeling of volatile organic compounds. 1. Emission inventory and validation. Environ. Sci. Technol. 27, 617–625.

Schnell, R.C., Oltmans, S.J., Neely, R.R., Endres, M.S., Molenar, J.V., White, A.B., 2009. Rapid photochemical production of ozone at high concentrations in a rural site during winter. Nat. Geosci. 2, 120–122.

Shah, T., Bar-Ilan, A., Grant, J., 2015. WRAP Phase III Oil and Gas Speciation Profiles. Ramboll Environ, Inc., Arlington, VA.

Skamarock, W.C., Klemp, J.B., Dudhia, J., Gill, D.O., Barker, D.M., Duda, M.G., Huang, X.-Y., Wang, W., Powers, J.G., 2005. A Description of the Advanced Research WRF Version 2. 113.

State of California Air Resources Board, 1997. ARB Aerosol Coatings Survey.

Swarthout, R.F., Russo, R.S., Zhou, Y., Hart, A.H., Sive, B.C., 2013. Volatile organic compound distributions during the NACHTT campaign at the Boulder Atmospheric Observatory: influence of urban and natural gas sources. J. Geophys. Res.: Atmosphere 118 (10), 614-610,637.

Thompson, C.R., Hueber, J., Helmig, D., 2014. Influence of oil and gas emissions on ambient atmospheric non-methane hydrocarbons in residential areas of Northeastern Colorado. Elementa: Science of the Anthropocene 2.

Toth, J.J., Johnson, R.H., 1985. Summer surface flow characteristics over northeast Colorado. Mon. Weather Rev. 113, 1458–1469.

Turner, M.C., Jerrett, M., Pope 3rd, C.A., Krewski, D., Gapstur, S.M., Diver, W.R., Beckerman, B.S., Marshall, J.D., Su, J., Crouse, D.L., Burnett, R.T., 2016. Long-term ozone exposure and mortality in a large prospective study. Am. J. Respir. Crit. Care Med. 193, 1134–1142.

U. S. EPA, 1998. Locating and Estimating Air Emissions from Sources of Benzene. Research Triangle Park, North Carolina.

U. S. EPA, 1999. Air Method, Toxic Organics-15 (TO-15): Compendium of Methods for the Determination of Toxic Organic Compounds in Ambient Air, Second Edition: Determination of Volatile Organic Compounds (VOCs) in Air Collected in Specially-Prepared Canisters and Analyzed by Gas Chromatography/Mass Spectrometry (GC/MS). Research Triangle Park, North Carolina.

U. S. EPA, 2009. Exhaust Emission Profiles for EPA SPECIATE Database: Energy Policy Act (EPAct) Low-Level Ethanol Fuel Blends and Tier 2 Light-Duty Vehicles, EPA 420-R-09-002. Research Triangle Park, North Carolina.

U. S. EPA, 2011. Meteorological Model Performance for Annual 2007 Simulations Meteorological Model Performance for Annual 2007 Simulations. Research Triangle Park, North Carolina.

U. S. EPA, 2012. Oil and natural gas sector: new source performance standards and national emissions standards for hazardous air pollutants reviews. Fed. Regist. 77, 49490–49600.

U. S. EPA, 2013. Regulatory Impact Analysis for the Final Revisions to the National Ambient Air Quality Standards for Particulate Matter. Research Triangle Park, North Carolina, pp. 1–474.

U. S. EPA, 2014. Motor Vehicle Emission Simulator (MOVES): User Guide for MOVES2014. US EPA. EPA-420-B-14-055.

U. S. Epa, 2016a. Oil and natural gas sector: emission standards for new, reconstructed and modified sources. Fed. Regist. 81, 35824–35942.

U. S. Epa, 2016b. SPECIATE Version 4.5 Database Development Documentation.

U. S. EPA, 2018. Green Book. Research Triangle Park, North Carolina.

Vos, T., Lim, S.S., Abbafati, C., Abbas, K.M., Abbasi, M., Abbasifard, M., Abbasi-Kangevari, M., Abbastabar, H., Abd-Allah, F., Abdelalim, A., Abdollahi, M., Abdollahpour, I., Abolhassani, H., Aboyans, V., Abrams, E.M., Abreu, L.G., Abrigo, M.R.M., Abu-Raddad, L.J., Abushouk, A.I., Acebedo, A., Ackerman, I.N., Adabi, M., Adamu, A.A., Adebayo, O.M., Adekanmbi, V., Adelson, J.D., Adetokunboh, O.O., Adham, D., Afshari, M., Afshin, A., Agardh, E.E., Agarwal, G., Agesa, K.M., Aghaali, M., Aghamir, S.M.K., Agrawal, A., Ahmad, T., Ahmadi, A., Ahmadi, M., Ahmadieh, H., Ahmadpour, E., Akalu, T.Y., Akinyemi, R.O., Akinyemiju, T., Akombi, B., Al-Aly, Z., Alam, K., Alam, N., Alam, S., Alam, T., Alanzi, T.M., Albertson, S.B., Alcalde-Rabanal, J.E., Alema, N.M., Ali, M., Ali, S., Alicandro, G., Alijanzadeh, M., Alinia, C., Alipour, V., Aljunid, S.M., Alla, F., Allebeck, P., Almasi-Hashiani, A., Alonso, J., Al-Raddadi, R.M., Altirkawi, K.A., Alvis-Guzman, N., Alvis-Zakzuk, N.J., Amini, S., Amini-Rarani, M., Aminorroaya, A., Amiri, F., Amit, A.M.L., Amugsi, D.A., Amul, G.G.H., Anderlini, D., Andrei, C.L., Andrei, T., Anjomshoa, M., Ansari, F., Ansari, I., Ansari-Moghaddam, A., Antonio, C. A.T., Antony, C.M., Antriyandarti, E., Anvari, D., Anwer, R., Arabloo, J., Arab-Zozani, M., Aravkin, A.Y., Ariani, F., Ärnlöv, J., Aryal, K.K., Arzani, A., Asadi-Aliabadi, M., Asadi-Pooya, A.A., Asghari, B., Ashbaugh, C., Atnafu, D.D., Atre, S.R., Ausloos, F., Ausloos, M., Ayala Quintanilla, B.P., Ayano, G., Ayanore, M.A., Aynalem, Y.A., Azari, S., Azarian, G., Azene, Z.N., Babaee, E., Badawi, A., Bagherzadeh, M., Bakhshaei, M.H., Bakhtiari, A., Balakrishnan, S., Balalla, S., Balassyano, S., Banach, M., Banik, P.C., Bannick, M.S., Bante, A.B., Baraki, A.G., Barboza, M.A., Barker-Collo, S.L., Barthelemy, C.M., Barua, L., Barzegar, A., Basu, S., Baune, B.T., Bayati, M., Bazmandegan, G., Bedi, N., Beghi, E., Béjot, Y., Bello, A.K., Bender, R.G., Bennett, D.A., Bennitt, F.B., Bensenor, I.M., Benziger, C.P., Berhe, K., Bernabe, E., Bertolacci, G.J., Bhageerathy, R., Bhala, N., Bhandari, D., Bhardwaj, P., Bhattacharyya, K., Bhutta, Z.A., Bibi, S., Biehl, M.H., Bikbov, B., Bin Sayeed, M.S., Biondi, A., Birihane, B.M., Bisanzio, D., Bisignano, C., Biswas, R.K., Bohlouli, S., Bohluli, M., Bolla, S.R.R., Boloor, A., Boon-Dooley, A.S., Borges, G., Borzì, A.M., Bourne, R., Brady, O.J., Brauer, M., Brayne, C., Breitborde, N.J.K., Brenner, H., Briant, P.S., Briggs, A.M., Briko, N.I., Britton, G.B., Bryazka, D., Buchbinder, R., Bumgarner, B.R., Busse, R., Butt, Z.A., Caetano dos Santos, F.L., Cámera, L.L.A.A., Campos-Nonato, I.R., Car, J., Cárdenas, R., Carreras, G., Carrero, J.J., Carvalho, F., Castaldelli-Maia, J.M., Castañeda-Orjuela, C.A., Castelpietra, G., Castle, C.D., Castro, F., Catalá-López, F., Causey, K., Cederroth, C.R., Cercy, K.M., Cerin, E., Chandan, J.S., Chang, A.R., Charlson, F.J., Chattu, V.K., Chaturvedi, S., Chimed-Ochir, O., Chin, K.L., Cho, D.Y., Christensen, H., Chu, D.-T., Chung, M.T.,

Cicuttini, F.M., Ciobanu, L.G., Cirillo, M., Collins, E.L., Compton, K., Conti, S., Cortesi, P.A., Costa, V.M., Cousin, E., Cowden, R.G., Cowie, B.C., Cromwell, E.A., Cross, D.H., Crowe, C.S., Cruz, J.A., Cunningham, M., Dahlawi, S.M.A., Damiani, G., Dandona, L., Dandona, R., Darwesh, A.M., Daryani, A., Das, J.K., Das Gupta, R., das Neves, J., Dávila-Cervantes, C.A., Davletov, K., De Leo, D., Dean, F.E., DeCleene, N. K., Deen, A., Degenhardt, L., Dellavalle, R.P., Demeke, F.M., Demsie, D.G., Denova-Gutiérrez, E., Dereje, N.D., Dervenis, N., Desai, R., Desalew, A., Dessie, G.A., Dharmaratne, S.D., Dhungana, G.P., Dianatinasab, M., Diaz, D., Dibaji Forooshani, Z. S., Dingels, Z.V., Dirac, M.A., Djalalinia, S., Do, H.T., Dokova, K., Dorostkar, F., Doshi, C.P., Doshmangir, L., Douiri, A., Doxey, M.C., Driscoll, T.R., Dunachie, S.J., Duncan, B.B., Duraes, A.R., Eagan, A.W., Ebrahimi Kalan, M., Edvardsson, D., Ehrlich, J.R., El Nahas, N., El Sayed, I., El Tantawi, M., Elbarazi, I., Elgendy, I.Y., Elhabashy, H.R., El-Jaafary, S.I., Elyazar, I.R.F., Emamian, M.H., Emmons-Bell, S., Erskine, H.E., Eshrati, B., Eskandarieh, S., Esmaeilnejad, S., Esmaeilzadeh, F., Esteghamati, A., Estep, K., Etemadi, A., Etisso, A.E., Farahmand, M., Faraj, A., Fareed, M., Faridnia, R., Farinha, C.S.e.S., Farioli, A., Faro, A., Faruque, M., Farzadfar, F., Fattahi, N., Fazlzadeh, M., Feigin, V.L., Feldman, R., Fereshtehnejad, S.-M., Fernandes, E., Ferrari, A.J., Ferreira, M.L., Filip, I., Fischer, F., Fisher, J.L., Fitzgerald, R., Flohr, C., Flor, L.S., Foigt, N.A., Folayan, M.O., Force, L. M., Fornari, C., Foroutan, M., Fox, J.T., Freitas, M., Fu, W., Fukumoto, T., Furtado, J. M., Gad, M.M., Gakidou, E., Galles, N.C., Gallus, S., Gamkrelidze, A., Garcia-Basteiro, A.L., Gardner, W.M., Geberemariyam, B.S., Gebrehiwot, A.M., Gebremedhin, K.B., Gebreslassie, A.A.A.A., Gershberg Hayoon, A., Gething, P.W., Ghadimi, M., Ghadiri, K., Ghafourifard, M., Ghajar, A., Ghamari, F., Ghashghaee, A., Ghiasvand, H., Ghith, N., Gholamian, A., Gilani, S.A., Gill, P.S., Gitimoghaddam, M., Giussani, G., Goli, S., Gomez, R.S., Gopalani, S.V., Gorini, G., Gorman, T.M., Gottlich, H.C., Goudarzi, H., Goulart, A.C., Goulart, B.N.G., Grada, A., Grivna, M., Grosso, G., Gubari, M.I.M., Gugnani, H.C., Guimaraes, A.L.S., Guimarães, R.A., Guled, R.A., Guo, G., Guo, Y., Gupta, R., Haagsma, J.A., Haddock, B., Hafezi-Nejad, N., Hafiz, A., Hagins, H., Haile, L.M., Hall, B.J., Halvaei, I., Hamadeh, R.R., Hamagharib Abdullah, K., Hamilton, E.B., Han, C., Han, H., Hankey, G.J., Haro, J. M., Harvey, J.D., Hasaballah, A.I., Hasanzadeh, A., Hashemian, M., Hassanipour, S., Hassankhani, H., Havmoeller, R.J., Hay, R.J., Hay, S.I., Hayat, K., Heidari, B., Heidari, G., Heidari-Soureshjani, R., Hendrie, D., Henrikson, H.J., Henry, N.J., Herteliu, C., Heydarpour, F., Hird, T.R., Hoek, H.W., Hole, M.K., Holla, R., Hoogar, P., Hosgood, H.D., Hosseinzadeh, M., Hostiuc, M., Hostiuc, S., Househ, M., Hoy, D.G., Hsairi, M., Hsieh, V.C.-r., Hu, G., Huda, T.M., Hugo, F.N., Huynh, C.K., Hwang, B.-F., Iannucci, V.C., Ibitoye, S.E., Ikuta, K.S., Ilesanmi, O.S., Ilic, I.M., Ilic, M.D., Inbaraj, L.R., Ippolito, H., Irvani, S.S.N., Islam, M.M., Islam, M., Islam, S. M.S., Islami, F., Iso, H., Ivers, R.Q., Iwu, C.C.D., Iyamu, I.O., Jaafari, J., Jacobsen, K. H., Jadidi-Niaragh, F., Jafari, H., Jafarinia, M., Jahagirdar, D., Jahani, M.A., Jahanmehr, N., Jakovljevic, M., Jalali, A., Jalilian, F., James, S.L., Janjani, H., Janodia, M.D., Jayatilleke, A.U., Jeemon, P., Jenabi, E., Jha, R.P., Jha, V., Ji, J.S., Jia, P., John, O., John-Akinola, Y.O., Johnson, C.O., Johnson, S.C., Jonas, J.B., Joo, T., Joshi, A., Jozwiak, J.J., Jürisson, M., Kabir, A., Kabir, Z., Kalani, H., Kalani, R., Kalankesh, L.R., Kalhor, R., Kamiab, Z., Kanchan, T., Karami Matin, B., Karch, A., Karim, M.A., Karimi, S.E., Kassa, G.M., Kassebaum, N.J., Katikireddi, S.V., Kawakami, N., Kayode, G.A., Keddie, S.H., Keller, C., Kereselidze, M., Khafaie, M.A., Khalid, N., Khan, M., Khatab, K., Khater, M.M., Khatib, M.N., Khayamzadeh, M., Khodayari, M.T., Khundkar, R., Kianipour, N., Kieling, C., Kim, D., Kim, Y.-E., Kim, Y.J., Kimokoti, R.W., Kisa, A., Kisa, S., Kissimova-Skarbek, K., Kivimäki, M., Kneib, C.J., Knudsen, A.K.S., Kocarnik, J.M., Kolola, T., Kopec, J.A., Kosen, S., Koul, P.A., Koyanagi, A., Kravchenko, M.A., Krishan, K., Krohn, K.J., Kuate Defo, B., Kucuk Bicer, B., Kumar, G.A., Kumar, M., Kumar, P., Kumar, V., Kumaresh, G., Kurmi, O.P., Kusuma, D., Kyu, H.H., La Vecchia, C., Lacey, B., Lal, D.K., Lalloo, R., Lam, J.O., Lami, F.H., Landires, I., Lang, J.J., Lansingh, V.C., Larson, S.L., Larsson, A. O., Lasrado, S., Lassi, Z.S., Lau, K.M.-M., Lavados, P.M., Lazarus, J.V., Ledesma, J.R., Lee, P.H., Lee, S.W.H., LeGrand, K.E., Leigh, J., Leonardi, M., Lescinsky, H., Leung, J., Levi, M., Lewington, S., Li, S., Lim, L.-L., Lin, C., Lin, R.-T., Linehan, C., Linn, S., Liu, H.-C., Liu, S., Liu, Z., Looker, K.J., Lopez, A.D., Lopukhov, P.D., Lorkowski, S., Lotufo, P.A., Lucas, T.C.D., Lugo, A., Lunevicius, R., Lyons, R.A., Ma, J., MacLachlan, J.H., Maddison, E.R., Maddison, R., Madotto, F., Mahasha, P.W., Mai, H.T., Majeed, A., Maled, V., Maleki, S., Malekzadeh, R., Malta, D.C., Mamun, A. A., Manafi, A., Manafi, N., Manguerra, H., Mansouri, B., Mansournia, M.A., Mantilla Herrera, A.M., Maravilla, J.C., Marks, A., Martins-Melo, F.R., Martopullo, I., Masoumi, S.Z., Massano, J., Massenburg, B.B., Mathur, M.R., Maulik, P.K., McAlinden, C., McGrath, J.J., McKee, M., Mehndiratta, M.M., Mehri, F., Mehta, K. M., Meitei, W.B., Memiah, P.T.N., Mendoza, W., Menezes, R.G., Mengesha, E.W., Mengesha, M.B., Mereke, A., Meretoja, A., Meretoja, T.J., Mestrovic, T., Miazgowski, B., Miazgowski, T., Michalek, I.M., Mihretie, K.M., Miller, T.R., Mills, E. J., Mirica, A., Mirrakhimov, E.M., Mirzaei, H., Mirzaei, M., Mirzaei-Alavijeh, M., Misganaw, A.T., Mithra, P., Moazen, B., Moghadaszadeh, M., Mohamadi, E., Mohammad, D.K., Mohammad, Y., Mohammad Gholi Mezerji, N., Mohammadian-Hafshejani, A., Mohammadifard, N., Mohammadpourhodki, R., Mohammed, S., Mokdad, A.H., Molokhia, M., Momen, N.C., Monasta, L., Mondello, S., Mooney, M. D., Moosazadeh, M., Moradi, G., Moradi, M., Moradi-Lakeh, M., Moradzadeh, R., Moraga, P., Morales, L., Morawska, L., Moreno Velásquez, I., Morgado-da-Costa, J., Morrison, S.D., Mosser, J.F., Mouodi, S., Mousavi, S.M., Mousavi Khaneghah, A., Mueller, U.O., Munro, S.B., Muriithi, M.K., Musa, K.I., Muthupandian, S., Naderi, M., Nagarajan, A.J., Nagel, G., Naghshtabrizi, B., Nair, S., Nandi, A.K., Nangia, V., Nansseu, J.R., Nayak, V.C., Nazari, J., Negoi, I., Negoi, R.I., Netsere, H.B.N., Ngunjiri, J.W., Nguyen, C.T., Nguyen, J., Nguyen, M., Nguyen, M., Nichols, E., Nigatu, D., Nigatu, Y.T., Nikbakhsh, R., Nixon, M.R., Nnaji, C.A., Nomura, S., Norrving, B., Noubiap, J.J., Nowak, C., Nunez-Samudio, V., Oţoiu, A., Oancea, B., Odell, C.M., Ogbo, F.A., Oh, I.-H., Okunga, E.W., Oladnabi, M., Olagunju, A.T., Olusanya, B.O., Olusanya, J.O., Oluwasanu, M.M., Omar Bali, A., Omer, M.O., Ong, K.L., Onwujekwe, O.E., Orji, A.U., Orpana, H.M., Ortiz, A., Ostroff, S.M., Otstavnov, N., Otstavnov, S.S., Øverland, S., Owolabi, M.O., P A, M., Padubidri, J.R., Pakhare, A.P., Palladino, R., Pana, A., Panda-Jonas, S., Pandey, A., Park, E.-K., Parmar, P.G.K., Pasupula, D.K., Patel, S.K., Paternina-Caicedo, A.J., Pathak, A., Pathak, M., Patten, S.B., Patton, G.C., Paudel, D., Pazoki Toroudi, H., Peden, A.E., Pennini, A., Pepito, V.C.F., Peprah, E.K., Pereira, A., Pereira, D.M., Perico, N., Pham, H.Q., Phillips, M.R., Pigott, D.M., Pilgrim, T., Pilz, T.M., Pirsaheb, M., Plana-Ripoll, O., Plass, D., Pokhrel, K.N., Polibin, R.V., Polinder, S., Polkinghorne, K.R., Postma, M.J., Pourjafar, H., Pourmalek, F., Pourmirza Kalhori, R., Pourshams, A., Poznańska, A., Prada, S.I., Prakash, V., Pribadi, D.R.A., Pupillo, E., Quazi Syed, Z., Rabiee, M., Rabiee, N., Radfar, A., Rafiee, A., Rafiei, A., Raggi, A., Rahimi-Movaghar, A., Rahman, M.A., Rajabpour-Sanati, A., Rajati, F., Ramezanzadeh, K., Ranabhat, C.L., Rao, P.C., Rao, S.J., Rasella, D., Rastogi, P., Rathi, P., Rawaf, D.L., Rawaf, S., Rawal, L., Razo, C., Redford, S.B., Reiner Jr., R.C., Reinig, N., Reitsma, M. B., Remuzzi, G., Renjith, V., Renzaho, A.M.N., Resnikoff, S., Rezaei, N., Rezai, M.s., Rezapour, A., Rhinehart, P.-A., Riahi, S.M., Ribeiro, A.L.P., Ribeiro, D.C., Ribeiro, D., Rickard, J., Roberts, N.L.S., Roberts, S., Robinson, S.R., Roever, L., Rolfe, S., Ronfani, L., Roshandel, G., Roth, G.A., Rubagotti, E., Rumisha, S.F., Sabour, S., Sachdev, P.S., Saddik, B., Sadeghi, E., Sadeghi, M., Saeidi, S., Safi, S., Safiri, S., Sagar, R., Sahebkar, A., Sahraian, M.A., Sajadi, S.M., Salahshoor, M.R., Salamati, P., Salehi Zahabi, S., Salem, H., Salem, M.R.R., Salimzadeh, H., Salomon, J.A., Salz, I., Samad, Z., Samy, A.M., Sanabria, J., Santomauro, D.F., Santos, I.S., Santos, J.V., Santric-Milicevic, M.M., Saraswathy, S.Y.I., Sarmiento-Suárez, R., Sarrafzadegan, N., Sartorius, B., Sarveazad, A., Sathian, B., Sathish, T., Sattin, D., Sbarra, A.N., Schaeffer, L.E., Schiavolin, S., Schmidt, M.I., Schutte, A.E., Schwebel, D.C., Schwendicke, F., Senbeta, A.M., Senthilkumaran, S., Sepanlou, S.G., Shackelford, K. A., Shadid, J., Shahabi, S., Shaheen, A.A., Shaikh, M.A., Shalash, A.S., Shams-Beyranvand, M., Shamsizadeh, M., Shannawaz, M., Sharafi, K., Sharara, F., Sheena, B.S., Sheikhtaheri, A., Shetty, R.S., Shibuya, K., Shiferaw, W.S., Shigematsu, M., Shin, J.I., Shiri, R., Shirkoohi, R., Shrime, M.G., Shuval, K., Siabani, S., Sigfusdottir, I.D., Sigurvinsdottir, R., Silva, J.P., Simpson, K.E., Singh, A., Singh, J.A., Skiadaresi, E., Skou, S.T.S., Skryabin, V.Y., Sobngwi, E., Sokhan, A., Soltani, S., Sorensen, R.J.D., Soriano, J.B., Sorrie, M.B., Soyiri, I.N., Sreeramareddy, C.T., Stanaway, J.D., Stark, B.A., Ştefan, S.C., Stein, C., Steiner, C., Steiner, T.J., Stokes, M.A., Stovner, L.J., Stubbs, J.L., Sudaryanto, A., Sufiyan, M.a. B., Sulo, G., Sultan, I., Sykes, B.L., Sylte, D.O., Szócska, M., Tabarés-Seisdedos, R., Tabb, K.M., Tadakamadla, S.K., Taherkhani, A., Tajdini, M., Takahashi, K., Taveira, N., Teagle, W.L., Teame, H., Tehrani-Banihashemi, A., Teklehaimanot, B.F., Terrason, S., Tessema, Z.T., Thankappan, K.R., Thomson, A.M., Tohidinik, H.R., Tonelli, M., Topor-Madry, R., Torre, A.E., Touvier, M., Tovani-Palone, M.R.R., Tran, B.X., Travillian, R., Troeger, C.E., Truelsen, T.C., Tsai, A.C., Tsatsakis, A., Tudor Car, L., Tyrovolas, S., Uddin, R., Ullah, S., Undurraga, E.A., Unnikrishnan, B., Vacante, M., Vakilian, A., Valdez, P.R., Varughese, S., Vasankari, T.J., Vasseghian, Y., Venketasubramanian, N., Violante, F.S., Vlassov, V., Vollset, S.E., Vongpradith, A., Vukovic, A., Vukovic, R., Waheed, Y., Walters, M.K., Wang, J., Wang, Y., Wang, Y.-P., Ward, J.L., Watson, A., Wei, J., Weintraub, R.G., Weiss, D.J., Weiss, J., Westerman, R., Whisnant, J.L., Whiteford, H.A., Wiangkham, T., Wiens, K. E., Wijeratne, T., Wilner, L.B., Wilson, S., Wojtyniak, B., Wolfe, C.D.A., Wool, E.E., Wu, A.-M., Wulf Hanson, S., Wunrow, H.Y., Xu, G., Xu, R., Yadgir, S., Yahyazadeh Jabbari, S.H., Yamagishi, K., Yaminfirooz, M., Yano, Y., Yaya, S., Yazdi-Feyzabadi, V., Yearwood, J.A., Yeheyis, T.Y., Yeshitila, Y.G., Yip, P., Yonemoto, N., Yoon, S.-J., Yoosefi Lebni, J., Younis, M.Z., Younker, T.P., Yousefi, Z., Yousefifard, M., Yousefinezhadi, T., Yousuf, A.Y., Yu, C., Yusefzadeh, H., Zahirian Moghadam, T., Zaki, L., Zaman, S.B., Zamani, M., Zamanian, M., Zandian, H., Zangeneh, A., Zastrozhin, M.S., Zewdie, K.A., Zhang, Y., Zhang, Z.-J., Zhao, J.T., Zhao, Y., Zheng, P., Zhou, M., Ziapour, A., Zimsen, S.R.M., Naghavi, M., Murray, C.J. L., 2020. Global burden of 369 diseases and injuries in 204 countries and territories, 1990–2019: a systematic analysis for the Global Burden of Disease Study 2019. Lancet 396, 1204–1222.

Watson, J.G., Cooper, J.A., Huntzicker, J.J., 1984. The effective variance weighting for least squares calculations applied to the mass balance receptor model. Atmos. Environ. 18, 1347–1355, 1967.

Wells, D., 2017. Consequences of the Evolution of Oil and Gas Control and Production Technology in the Denver Ozone Nonattainment Area, 2017 International Emissions Inventory Conference. Baltimore, MD.

Yarwood, G., Rao, S., Yocke, M., Whitten, G., 2005. Updates to the Carbon Bond Chemical Mechanism: CB05 Final Report to the. US EPA.

Zhang, Y., Sheesley, R.J., Schauer, J.J., Lewandowski, M., Jaoui, M., Offenberg, J.H., Kleindienst, T.E., Edney, E.O., 2009. Source apportionment of primary and secondary organic aerosols using positive matrix factorization (PMF) of molecular markers. Atmos. Environ. 43, 5567–5574.

Zhao, S., Russell, M.G., Hakami, A., Capps, S.L., Turner, M.D., Henze, D.K., Percell, P.B., Resler, J., Shen, H., Russell, A.G., Nenes, A., Pappin, A.J., Napelenok, S.L., Bash, J. O., Fahey, K.M., Carmichael, G.R., Stanier, C.O., Chai, T., 2020. A multiphase CMAQ version 5.0 adjoint. Geosci. Model Dev. 13, 2925–2944.